THERMAL DRIFT IN CONVECTIVE MICROMACHINED ACCELEROMETERS

by

Andy Bo Wu

B., Eng, Wuhan Institute of Technology, 2002

A THESIS SUBMITTED IN PARTIAL FULFILLMENT
OF THE REQUIREMENTS FOR THE DEGREE OF
MASTER OF APPLIED SCIENCE
in the School
of
Engineering Science

© Andy Bo Wu 2007
SIMON FRASER UNIVERSITY
2007

APPROVAL

Name: Andy Bo Wu

Degree: Master of Applied Science

Title of thesis: Thermal Drift in Convective Micromachined Accelerometers

Examining Committee: Dr. Ivan V. Bajic,
Assistant Professor, Engineering Science
Simon Fraser University
Chair

Dr. John D. Jones,
Associate Professor, Engineering Science
Simon Fraser University
Senior Supervisor

Dr. Albert M. Leung,
Professor, Engineering Science
Simon Fraser University
Supervisor

Dr. Ash M. Parameswaran,
Professor, Engineering Science
Simon Fraser University
SFU Examiner

Date Approved: Aug 1, 2007

SFU SIMON FRASER UNIVERSITY
LIBRARY

Declaration of
Partial Copyright Licence

Abstract

The field of micromachined accelerometers is reviewed. A convection-based micromachined accelerometer without moving elements, based on the buoyancy of a heated fluid around a polysilicon heater, has previously been developed and reported. Significant features of this class of accelerometer include low cost and the combination of high sensitivity with high survivability. However, one of its big disadvantages is thermal drift: the sensitivity changes rapidly as the ambient temperature changes. A recent numerical and experimental study has shown that the sensitivity of the convective accelerometer is a function of the Rayleigh number of the working fluid. Using this criterion, a few liquids are selected as potential working fluids to improve the sensitivity and stability of the accelerometer. The Computational Fluid Dynamics (CFD) program 'FLOTRAN' is used to model the accelerometer performance using each of these fluids. Based on FLOTRAN modeling, some fluids are selected for experimental investigation. The thermal drift of the accelerometer using different working fluids is documented and the reasons for this thermal drift determined. Based on this observation, some possible solutions are proposed to reduce or eliminate the thermal drift.

Acknowledgments

I am deeply indebted to my senior supervisor, Dr. John Jones, for his constant support, inspiration and encouragement. Without his help, this work would not be possible.

I would like to thank Dr. Albert Leung and Dr. Ash Parameswaran who introduced me to the wonderful world of accelerometers. Their insightful advice and great patience is much appreciated.

I would also like to thank all my friends in the School of Engineering Science. They are: Fuhan, Haibo, Michael, Leo, Maggie, Jinyun, Qing, Jingyun, Kourosh and others. I will never forget these three years of beautiful memories at Simon Fraser University.

Especially, I would like to give my special thanks to my wife Ashley, my mom and dad whose patient love enabled me to complete this work.

Nomenclature

T_i, T_o: the temperature of the inner and outer cylinder, respectively (K)

r_i, r_o: the radius of the inner cylinder and the outer cylinder, respectively (m)

R: the radius ratio, $R = r_o/r_i$

c: specific heat $(J/kg.K)$

ρ: density of the fluid (kg/m^3)

β: the thermal expansion coefficient (K^{-1})

μ: dynamic viscosity $(Pa.s)$

k: thermal conductivity $(W/m.K)$

$\triangle T$:   the temperature difference between the inner cylinder and outer cylinder (K)

τ: the characteristic response time (s)

ρ_c: the density of the thermocouple material (kg/m^3)

V_c: the volume of thermocouple (m^3)

c_c: the specific heat of thermocouple $(J/kg.K)$

h: the convective heat transfer coefficient $(W/m^2.K)$

A_c: the surface area of thermocouple (m^2)

l: characteristic length of heater (m)

Q: the power passed through the polysilicon heater (W)

A: the area of heating element (m^2)

S_i: the sensitivity at the initial temperature $(\mu V/g)$

S_f: the sensitivity at the final temperature $(\mu V/g)$

T_i, T_f: the initial and final temperatures, respectively (K)

α: thermal diffusivity of the fluid, $\alpha = \frac{k}{\rho c}$ (m^2/s)

Pr: Prandtl number, $Pr = \frac{\mu c}{k}$

Ra: Rayleigh number, $Ra = \frac{c\rho^2 r_i^3 g \triangle T \beta}{\mu k}$

F_0:   Fourier number, $F_0 = \frac{\tau \alpha}{r_i}$

$A.T.$:   ambient temperature (K)

$S.T.$:   the sensitivity of accelerometers $(^\circ C/g)$

$R.T.$:   response time (s)

MDT: Maximum Differential Temperature (K)

Contents

List of Tables

List of Figures

Chapter 1

Introduction to Micromachined Accelerometers

An accelerometer is a transducer which converts acceleration into an electrical signal proportional to the acceleration. Many kinds of micromachined accelerometers have been applied in different fields, including navigation systems, military applications, automobile industry and consumer electronics [1]. In the past few years, the application of accelerometers has been extended from industry to ordinary consumer electronics, such as detection of shake in digital cameras and in gaming consoles for detecting movement of the game controller.

Conventional micromachined accelerometers work by sensing the displacement of a proof mass or the deflection of a cantilever beam. Those accelerometers have been developed for many years and their performance has become better and better. Some conventional accelerometers, including capacitive accelerometers and piezoresistive accelerometers, are introduced in this chapter. The common feature of these two different class of accelerometers is that they have a movable proof mass. Recently, a novel micromachined accelerometer without proof mass has been reported [3]. Compared to traditional accelerometers, this class of convection-based microthermal accelerometer features small size, low cost, high sensitivity and high survivability.
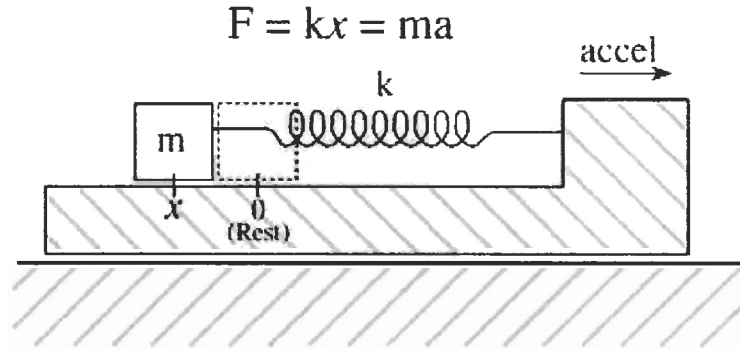
Figure 1.1: The Model of Proof-Mass-Based Accelerometer

1.1   Some Conventional Micromachined Accelerometers

There are many conventional accelerometers which sense accelerations by detecting the displacement of a proof mass, say capacitive accelerometer, or the change in resistance due to compression, say piezoresistive accelerometer. The model of proof-mass-based accelerometer is shown in Figure 1.1.

The proof mass stays at the position O when no acceleration is applied to the accelerometer in the direction of spring. When an acceleration is applied to the accelerometer, the mass moves a distance x to its left. One assumption is that there is no friction between the mass and plate. Due to the acceleration, the spring is extended by the proof mass until the forces are balanced. Equation (1.1) is then satisfied. Meanwhile, from Equation (1.2), the acceleration can be deduced from the distance the proof mass moved.

$$F = k \cdot x = m \cdot a \tag{1.1}$$

$$a = \frac{k}{m} \cdot x \tag{1.2}$$

where:

k: the spring constant

x: the distance by which spring is elongated

m: the mass of the object
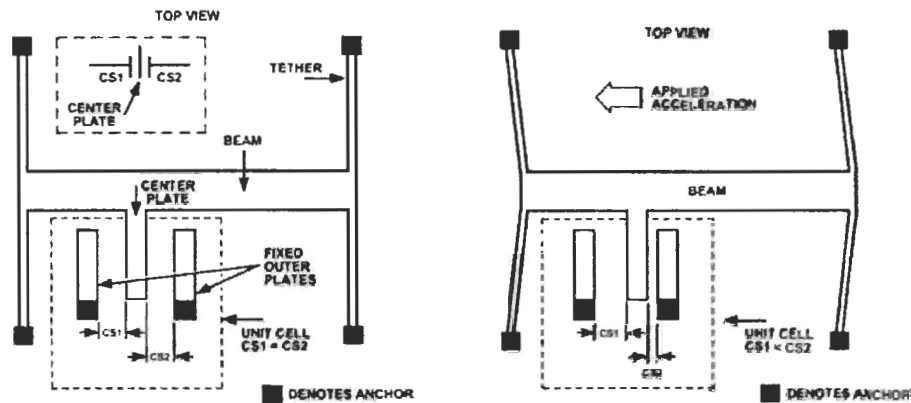
Figure 1.2: The Schematic of Design Principle – ADXL50

1.1.1 Capacitive Accelerometers

The capacitive accelerometer senses acceleration by sensing capacitance change due to displacement of a proof mass. Two micromachining technologies allow different applications of capacitive accelerometers. The capacitive accelerometer based on bulk micromachining technologies features very high resolution but is expensive. The capacitive accelerometer based on surface micromachining features low-cost mass fabrication. The latter design is widely used in air-bag control systems [9].

Based on the working theory illustrated in Figure 1.1, a commercial capacitive accelerometer ADXL50 has been fabricated by using surface micromachining technologies. The design principle of the surface-micromachining-based capacitive accelerometer is shown in Figure 1.2. The capacitance is proportional to the area of conducting plates and the permittivity of the dielectric substance, and inversely proportional to the distance between the plates. In this design, the applied acceleration can be deduced from the capacitance change caused by the change in separation between the center plate and the outer plates.

Compared to single-sided capacitive sensing, the differential capacitive accelerometer shown in Figure 1.2 has two advantages:

- Better linear response can be achieved.

- Common voltage noise fluctuation is canceled out.

The left-side picture in Figure 1.2 shows a simplified view of one unit cell of the ADXL50 at rest. The actual structure contains 42 unit cells and a common movable beam. The sensor's fixed capacitor plates are driven differentially by a 1 MHz square wave: the two square wave amplitudes are equal with 180° phase difference. The signal output is 0 when the distance between the center plate and either side of fixed plates is the same, i.e., no acceleration experienced by the accelerometer.

When an acceleration is applied to the sensor, the central movable beam moves closer to one fixed plate and further from the other plate. In this case, a differential capacitance is generated and its magnitude is proportional to the applied acceleration. To achieve maximum sensitivity, the capacitive accelerometer should be positioned so that the direction of moving beam is aligned with the expected direction of acceleration.

1.1.2 Piezoresistive Accelerometer

The transducting element in piezoresistive accelerometers is a piezoresistor. The piezoresistor is an electrical resistor the resistance of which can change due to applied mechanical stress. The applied acceleration can be deduced from the resistance change of embedded piezoresistors.

The two most popular designs for piezoresistive accelerometers are cantilever beam-mass structures and quad-beam-mass structures [9]. One simplified view of a cantilever beam-mass structure is shown in Figure 1.3. To achieve higher sensitivity and linearity, a Wheatstone bridge containing four piezoresistors can be used to replace the single piezoresistor design.

The working theory of piezoresistive accelerometer is relatively simple. When an acceleration is applied in the direction normal to the frame of the chip, the beam which connects the frame and the mass is deflected due to the inertial force. The resistance of piezoresistor is changed and the applied acceleration is deduced from the signal output.
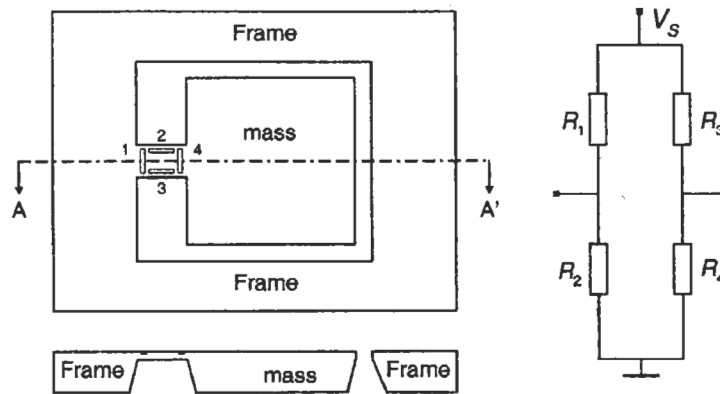
Figure 1.3: The Schematic of Piezoresistive Accelerometer

The early piezoresistive accelerometers suffer from two problems: lack of over-range protection and difficulty in damping control [9]. The response of piezoresistive accelerometer is either a short-lived fast-varying signal in the over-damped condition or an alternating signal in the slightly damped condition. The damping effect can be controlled by using squeeze-film air damping. To achieve high sensitivity of piezoresistive accelerometer, the beam should be thin, narrow and the seismic mass large. However, the beam is then easily broken if the applied acceleration is over its measuring range.

1.2 Some Unconventional Micromachined Accelerometers

1.2.1 Convection-Based Micromachined Accelerometer

The design principle of the convection-based micromachined accelerometer is shown in Figure 1.4. First, a few milli-amps electrical current is passed through a centrally placed polysilicon heater. A symmetric temperature profile is generated around the heater when no acceleration is applied parallel to the x-axis. As shown by the solid line, there is no temperature difference between the temperature sensors which are symmetrically located on either side of the heater.

When an acceleration is applied, the heated fluid around the heater will move in the same direction as the acceleration. In this case, the temperature profile is disturbed by the buoyancy force so that a differential temperature is produced between the sensors. The convective
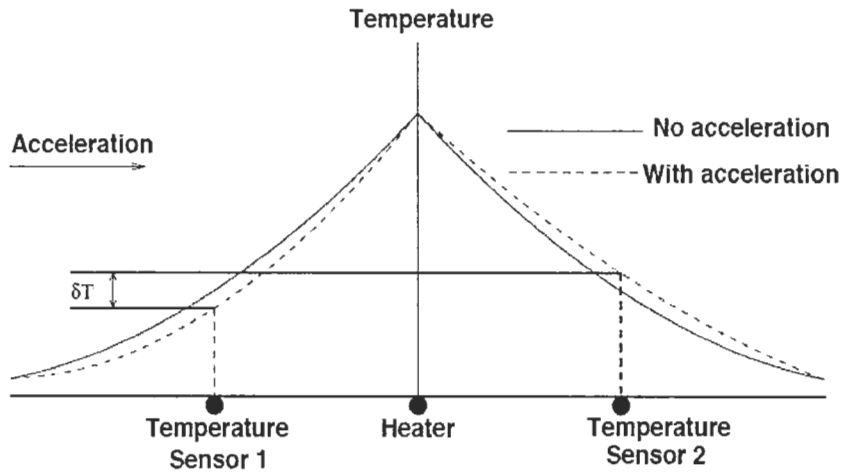
Figure 1.4: Illustration of the Operating Principle of a Convective Accelerometer

accelerometer can be used to detect static acceleration, such as gravitational acceleration, and dynamic acceleration, such as vibration and crash.

One significant advantage of convection-based micromachined accelerometer over the micro-electro-mechanical accelerometer is high survivability. The only moving element inside the convective accelerometer is a heated fluid around the polysilicon heater, which means it can resist much higher acceleration than the conventional accelerometer with proof mass. Proof-mass-based accelerometers break in the same way that they respond to acceleration – so there is a trade-off between sensitivity and survivability. Another advantage is that convective accelerometers are sensitive to small accelerations.

As reported in the prior literature [8], the sensitivity of the convective accelerometer can easily be up to 100 mV/g when using air as the working fluid. This can be compared to the conventional capacitive accelerometer, say ADXL50, with a sensitivity of 20 mV/g. Attempting to increase the conventional accelerometer's sensitivity by increasing the displacement of the proof mass or using thinner fingers will increase the size, cost and fragility of the device. The sensitivity of convective accelerometer can be increased two or three orders of magnitudes by using some liquids as the working fluid, which motivates the current work – Analysis of Liquid-Filled Convective Micromachined Accelerometer.
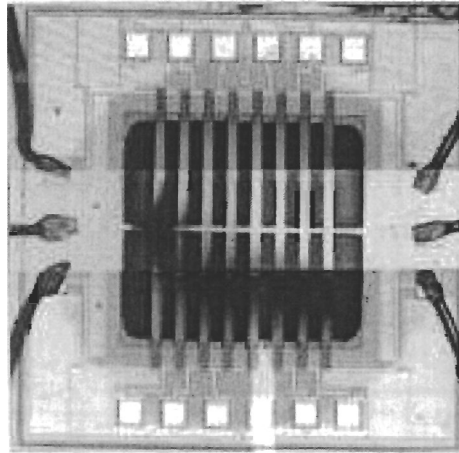
Figure 1.5: A Photograph of a Convective Accelerometer Chip

1.2.2 The Chip Structure

The structure of a test chip produced by MEMSIC® Corporation is shown in Figure 1.5. A 230 μm deep cavity is etched in a silicon wafer. It is 970 μm long in the direction parallel to the heater and 915 μm long in the orthogonal direction. A polysilicon heater bridge is located in one direction, and other eight sensor bridges are symmetrically located on the either side of the heater. The position of thermocouple junctions was defined by the position where the maximum differential temperature occurs and was fabricated by micromachining process. During operation, the chip is covered by a metal cap, giving a clearance of about 1000 μm above the heater plane. This chip was used in some of the experimental work described in Chapter 4.

Threshold of Detectability

The convection-based micromachined accelerometer is very sensitive to small accelerations so that it can be used as an inclinometer. As analyzed in Chapter 3, the sensitivity of convective accelerometer can be further improved two or three orders of magnitudes by using some liquids, say methanol.

Survivability

There is no moving element in the design of the convective accelerometer. Data provided by the convective accelerometer manufacturing corporation MEMSIC indicates that this class of accelerometers can withstand up to 50,000 g of acceleration or shock. Because of the mechanical structure of capacitive accelerometer, the maximum measuring range ADXL50 can survive is around 2000 g.

Thermal Drift

A critical feature of any measuring instrument is the change in its sensitivity with ambient temperature. Theoretical calculations and numerical simulations indicate that both the gas-filled and liquid-filled microthermal accelerometer suffer from thermal drift. The objective of this study is to determine the amount of thermal drift for different working fluids, and if possible, find means to minimize this drift. The other simplified version of convective accelerometer, convection-based micromachined accelerometer without thermopiles, is introduced and its performance will be evaluated in Chapter 3.

1.2.3 Thermal Proof-Mass Accelerometer

Another innovative design of micromachined accelerometer, also know as a thermal proof-mass accelerometer, has been proposed [11]. The cross section of such a thermal accelerometer is shown in Figure 1.6. In the figure, T_0 is the temperature of a heat sink, T_1 is the temperature of a heated plate, M_1 and M_2 are the distances between the heated plate and heat sink. The arrows show heat flow.

The main mechanism in which heat is transferred between the heated plate and heat sink is conduction. The principle is that the heat flux transferred from the heated plate to the heat sinks is inversely proportional to the gap distance M_1 and M_2, and proportional to the temperature difference between them [12]. The temperature difference caused by the displacement of heated plate can be measured by the thermopile and the applied acceleration is then determined. Some experiments were reported on the prototype accelerometers. The results are in reasonable agreement with theoretical calculations. However, we note that, since this design uses a proof mass, it suffers from the same trade-off between sensitivity and survivability as other proof-mass-based designs.
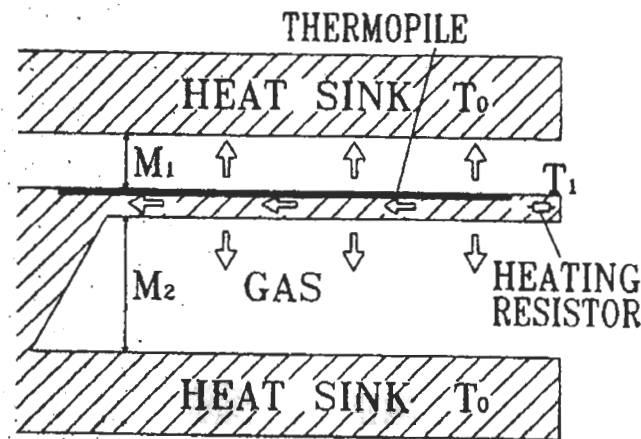
Figure 1.6: Cross Section of a Thermal Proof-Mass Accelerometer [12]

1.3 Application

In the accelerometer history, its most popular application is the air bag deployment in automobiles. It is also the main reason driving the accelerometer development and rapid cost drop. Recently, accelerometers are widely used in many military fields and consumer electronics. The main applications of accelerometers can be classified into the following three categories.

1.3.1 Inertial Measurement of Velocity and Position

The single-axis accelerometer can be used to measure velocity of moving objects. In the virtual golf simulator, there is an accelerometer in the golf club. Every time the player swings the golf club, the swing speed is deduced from the accelerometer.

The position change can be deduced from a three-axis accelerometer. The latest gaming consoles, Nintendo® Wii and PlayStation® 3, both incorporated accelerometers in their game controllers such that all games look more enjoyable. Also, an accelerometer embedded in a GPS system (Global Positioning System) can deduce position change even if the area is not covered by satellite signal or bad signal reception, such as in a tunnel.

1.3.2 Vibration and Shock Measurement

As mentioned, accelerometers are used in automobiles for air bag deployment. A further application in automobiles is that the convective accelerometer can be used in the vehicle's security system. The accelerometer can sense the vibration and this can linked to an alarm system as an anti-theft device. Two makes of laptop (IBM® and Apple®) now embed an accelerometer to control the magnetic head of the hard disk. If the accelerometer senses the laptop is falling, the magnetic head will move off the hard disk so that important data in the hard disk will not be corrupted.

1.3.3 Measurement of Gravity to Determine Orientation

Accelerometers have the ability to measure static accelerations, such as gravity. Due to high sensitivity of the convective accelerometer, it can be an inclinometer to detect the angle change.

1.4 Conclusion

In this chapter, a few conventional accelerometers have been introduced. Capacitive accelerometers and piezoresistive accelerometers both have application in different fields. Some relatively new designs of accelerometers are introduced and analyzed. The convection-based micromachined accelerometer was introduced and its performance was compared with other conventional accelerometers. Meanwhile, another innovative design, the thermal proof-mass accelerometer based on conduction was described.

The working theory of convection-based micromachined accelerometer was explained. Some prior literature indicates that the convective accelerometer has some advantages over conventional accelerometers, such as high sensitivity and survivability. The research object in this work is to document the thermal drift by using different working fluids.

Chapter 2

Convective Accelerometer −
Dimensional Analysis

In this chapter, the convection-based microthermal accelerometer, shown in Figure 1.5, is modeled as an infinitely long, horizontal, pair of concentric cylinders. The temperature distribution between the concentric cylinders, deduced by Hodnett [10], shows that the sensitivity of microthermal accelerometer is proportional to the Rayleigh number. A few fluids were carefully selected as potential working fluids and their physical properties at defined temperature were documented.

Based on the definition of Rayleigh number, a few possible methods are proposed to improve the sensitivity of the convection-based microthermal accelerometer. The main reasons for the thermal drift of convective accelerometer are analyzed, and a few solutions are proposed to reduce or eliminate this drift. The Prandtl number of selected working fluids were calculated and some conclusions were drawn about the response time of different working fluid-filled convective accelerometers.

2.1 Hodnett's Solution

To analyze the performance of the convective accelerometer, a mathematical model is created. The model is shown in Figure 2.1. The inner cylinder stands for the polysilicon heater and the outer cylinder for the cavity of the convective accelerometer. The temperature
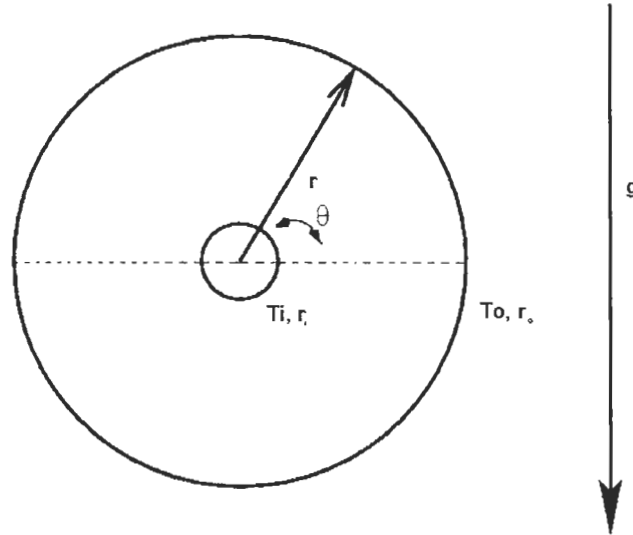
Figure 2.1: The Mathematical Model of Convective Accelerometer

sensors located to either side of the polysilicon heater are not represented in this model. Instead, the best position for temperature sensors will be deduced from the solution of temperature distribution.

In the coordinate system of Figure 2.1,

T_i, r_i: the temperature and radius of inner cylinder, respectively

T_o, r_o: the temperature and radius of outer cylinder, respectively

r: the dimensionless distance along the radius

θ: the angle between a given radius and the axis of acceleration

g: the acceleration applied to the model

A few assumptions are made to solve the governing equations. The complete procedures are described in Appendix I. Hodnett solved the governing equations by using perturbation

methods. The solution for the temperature distribution is shown in Equation (2.1).

$$\frac{T}{T_o} = 1 + \varepsilon f_1(r) + m\varepsilon^2 f_2(r) + Ra\varepsilon f_3(r)\sin(\theta) + o(m\varepsilon^2, Ra\varepsilon) \tag{2.1}$$

where:

T_o: the temperature of the outer cylinder

ε: the temperature difference between the cylinders divided by the temperature of the outer cylinder, $\varepsilon = \frac{T_i - T_o}{T_o}$

m: the parameter in $k \propto T^m$, in this study we assume $m = 0$

Ra: Rayleigh number

R: the radius ratio, $R = r_o/r_i$

And $f_1(r), f_2(r), f_3(r)$ are dimensionless functions of r and R only.

2.1.1 Sensitivity

Based on Lin's thesis [8], the dimensionless differential temperature, $\frac{\delta T}{T_o}$, measured by the accelerometer corresponds to the fourth term in Equation (2.1), $Ra\varepsilon f_3(r)\sin(\theta)$. Hence, the differential temperature for radially opposite points at a given r is:

$$\delta T = 2RaT_0\varepsilon f_3(r) \tag{2.2}$$

Equation (2.2) implies that the sensitivity of this convection-based accelerometer is proportional to the Rayleigh number. ε, which is the temperature difference between cylinders divided by the temperature of the outer cylinder, can be substituted in Equation (2.2), which becomes:

$$\delta T = 2Ra\triangle T f_3(r) \tag{2.3}$$

One important observation from Equation (2.3) is that the position of maximum differential temperature is independent of selected working fluids; this confirms that an accelerometer originally fabricated to use air as the working fluid **can** be used with a liquid working fluid.

Rayleigh number, which is the product of Grashof number and Prandtl number, can be expressed as:

$$Ra = \frac{c\rho^2 r_o^3 g \triangle T \beta}{\mu k} \tag{2.4}$$

where:

c: specific heat $(J/kg.K)$

ρ: density of the fluid (kg/m^3)

μ: dynamic viscosity $(Pa.s)$

k: thermal conductivity $(W/m.K)$

β: the thermal expansion coefficient (K^{-1})

$\triangle T$: the temperature difference between the inner cylinder and outer cylinder (K)

r_o: the radius of the outer cylinder (m). Hodnett defines a Rayleigh number based on the inner-cylinder radius, so his function $f_3(r)$ differs from that used in Equation (2.2) by a factor of R^3.

The solution for temperature distribution, Equation (2.3), suggests that a few methods could be used to improve the sensitivity of convection-based microthermal accelerometer.

Method 1: Select a Working Fluid with Higher Density

Some gases with higher molecular weight, and many liquids, could be potential working fluids to improve the sensitivity of the convection-based micromachined accelerometer. The sensitivity of convective accelerometer filled with gaseous working fluids can be improved if the gas in the cavity is pressurized so that its density increases. Theoretical calculations indicate that the sensitivity of the convective accelerometer can be improved two or three orders of magnitude if some liquid, say methanol, is selected as the working fluid.

Method 2: Increase $\triangle T$

The temperature difference between the cylinders can be increased by increasing the power for the polysilicon heater. One drawback is that the power consumption for the microthermal accelerometer is increased too. In addition, some prior literature [8] indicates that the performance of microthermal accelerometer filled with liquid working fluid becomes unstable if the heater temperature is higher than the boiling point of the liquid.

Method 3: Increase the dimension of r_o

The expression for Rayleigh number also suggests that larger radius of outer cylinder can

improve the sensitivity of the convective accelerometer. But the results of numerical simulations suggest that the sensitivity improvement is small. In addition, this increases the fabrication cost and power consumption of accelerometer.

All the above proposals are verified by theoretical calculations in this chapter. Then some simulations are conducted in the next chapter to confirm our predictions. We also try to determine the factors which cause thermal drift in the convective accelerometer by doing some theoretical calculations and numerical simulations.

2.1.2 Response Time

Response time, another important parameter of convection-based microthermal accelerometer, is the time taken for the signal to reach 63% of its maximum value. It results from two factors: the time taken for the differential temperature to establish itself, and the time taken for the thermocouples to respond to this differential. All the possible working fluids for the microthermal accelerometer can be classified into three categories according to their Prandtl number:

- Low-Prandtl-number working fluids, such as mercury

- Intermediate-Prandtl-number working fluids, such as air

- High-Prandtl-number working fluids, such as isopropanol

Prandtl number, one dimensionless characteristic of the working fluid, is the ratio of a fluid's ability to transport momentum to its ability to transport heat. The Prandtl number of any fluid is defined by Equation (2.5).

$$Pr = \frac{\mu c}{k} \tag{2.5}$$

Lin's research [8] shows that both thermocouple response time and thermal response time contribute to the overall response time of gas-filled microthermal accelerometer. However, as will be seen from the calculations later in this chapter, in the liquid-filled convective accelerometer, thermocouple response time made a negligible contribution.

Some empirical correlations [8] deduced from FLOTRAN simulations are used to calculate the thermal response time of different working-fluid-filled convective accelerometers.

F_0 in the following equations stands for Fourier number, $F_0 = \frac{\tau\alpha}{r_i}$, where α is the thermal diffusivity of the fluid, $\alpha = \frac{k}{\rho c}$.

- Empirical Correlation for Low-Prandtl-Number Working Fluids

$$\frac{F_0 Pr}{R^2} = \exp(-3.716597 - \frac{2.618219}{R} + 0.025842\ln(R)) \tag{2.6}$$

- Empirical Correlation for Intermediate-Prandtl-Number Working Fluids

$$\frac{F_0}{R^2} = \exp(-1.91326 - \frac{2.69773}{R} - 0.09997\ln(R)) \tag{2.7}$$

- Empirical Correlation for High-Prandtl-Number Working Fluids

$$\frac{F_0}{R^2} = \exp(-2.234524 - \frac{2.410128}{R} - 0.185096\ln(R)) \tag{2.8}$$

The thermal response time for different Prandtl number working fluid-filled convective accelerometer at defined temperature was calculated and some conclusions are drawn. The thermocouple response time was calculated by using Equation (2.9).

$$\tau_c = \frac{\rho_c V_c c_c}{h A_c} \tag{2.9}$$

where:

ρ_c: the density of the thermocouple material (kg/m^3)

V_c: the volume of thermocouple (m^3)

c_c: the specific heat of thermocouple $(J/kg.K)$

h: the convective heat transfer coefficient $(W/m^2 K)$

A_c: the surface area of thermocouple (m^2)

2.1.3 Thermal Drift

A critical feature of any measuring instrument is the change in its sensitivity with ambient temperature, referred to as 'thermal drift'. Both gas-filled and liquid-filled convective accelerometers suffer from thermal drift. One main objective in this work is to document the thermal drift of convection-based microthermal accelerometer using different working fluids. Meanwhile, we will propose a few solutions to reduce, or ideally, eliminate this drift. Some

theoretical calculations were done in this chapter to discover the reason of thermal drift. The results were verified by numerical simulations in the next chapter. To further confirm our hypotheses, the performance of a convective accelerometer using some working fluids was measured. Also, another accelerometer prototype was built to be used with electrically conductive working fluids and its performance was tested.

2.2   The Improvement of Sensitivity

The sensitivity of convective accelerometer is the change in convective accelerometer output (μV or mV) for an imposed acceleration. The definition of Rayleigh number suggests that a few methods can be used to improve the sensitivity of microthermal accelerometers.

As a basis for comparing the sensitivity and response time of different working fluids, a few assumptions are made.

- The applied acceleration is one g, which can be achieved by tilting the accelerometer from horizontal to vertical position.

- The radius of inner and outer cylinder is 100 μm and 1000 μm, respectively.

- The temperature difference between the inner cylinder and outer cylinder is 10 K.

2.2.1   Density Factor

Gas Working Fluids

Air is a good working fluid for convection-based micromachined accelerometer. It is non-corrosive, stable, and cheap. The sensitivity can be improved by selecting other suitable gas working fluids which have higher molecular weight. Two solutions have been employed to improve the sensitivity of convective accelerometer by using gases as the working fluids.

FIRST, a gas working fluid with higher molecular weight can get higher sensitivity. For comparison, another two denser gases, carbon dioxide (CO_2) and sulfur hexafluoride (SF_6), are selected as potential working fluids and their physical properties at 293 K are shown in Table 2.1. Based on the Rayleigh number calculated in Table 2.2, the sensitivity of

Table 2.1: Physical Properties of Some Selected Gas Working Fluids @ 293 K

	$C_p(J/Kg.K)$	$\rho(Kg/m^3)$	$\beta(K^{-1})$	$\mu(Kg/m.s)$	$k(W/m.K)$
Air	1,006	1.1774	3.32e-3	1.983e-5	0.02624
CO_2	871	1.7973	3.32e-3	1.496e-5	0.01657
SF_6	597	6.1300	3.32e-3	1.610e-5	0.01200

microthermal accelerometer using CO_2 and SF_6 is about 5 and 50 times of convective accelerometer using air as the working fluid, respectively. Response times (R.T.) in this table include the thermocouple response time calculated from Equation (2.9).

Table 2.2: Calculated Response Time and MDT of Selected Gas Working Fluids @ 293K

	$\alpha(m^2/s)$	**Prandtl**	**R.T. (s)**	**Rayleigh**	**MDT(K)**
Air	0.21e-4	0.71	0.634e-2	9.96e-4	0.0029
CO_2	0.11e-4	0.79	1.014e-2	37.00e-4	0.0107
SF_6	0.33e-5	0.81	2.912e-2	386.00e-4	0.1115

SECOND, higher pressure of a constant cavity volume can increase the density, and hence the sensitivity of microthermal accelerometer. The density of air is increased if we sealed the cavity of microthermal accelerometer at 1, 4, 8 and 10 times standard atmosphere. These hypotheses will be confirmed in the next chapter.

Liquid Working Fluids

Another immediate solution that comes to mind is that we can choose some liquid, which will have a density much higher than gas, to greatly increase the sensitivity of convective accelerometer. In this work, a few working fluids are carefully selected as the potential working liquids to improve the sensitivity of microthermal accelerometer. The physical properties of those working fluids at 293 K are listed in Table 2.3 and their corresponding Rayleigh numbers are also calculated. The results indicate that the sensitivities of convective accelerometer using liquid working fluids are from 10 to 1000 times higher than the accelerometer using air as the working fluid.

Table 2.3: Physical Properties of Selected Liquid Working Fluids @ 293 K

	C_v	ρ	β	μ	k	**Ra**	**MDT**
(unit)	$J/Kg.K$	Kg/m^3	K^{-1}	$Kg/m.s$	$W/m.K$	n/a	K
DI Water	4,182	1,000	0.18e-3	1.002e-3	0.597	12.40e-2	0.3561
Ethylene Glycol	2,382	1,117	0.65e-3	21.400e-3	0.249	3.56e-2	0.1028
Glycerine	2,386	1,264	0.50e-3	0.002e-3	0.284	4.41e-4	0.0012
Isopropanol	2,533	785	1.12e-3	2.396e-3	0.136	0.53	1.5210
Methanol	2,406	791	1.12e-3	0.585e-3	0.204	1.39	4.0040
Mercury	139.4	13,579	1.82e-4	1.550e-3	8.690	3.40e-2	0.0982

2.2.2 Power Factor

Theoretically, the higher the temperature difference between the cylinders, the higher sensitivity the accelerometer can achieve. But considering the boiling point of some liquid working fluids, the performance of convective accelerometer becomes unstable when the heater temperature becomes close to or higher than boiling point of liquids. More important for the accelerometer as an embedded portable device, power consumption is a parameter which can not be neglected. Therefore, increasing the sensitivity by increasing heater temperature will always induce a trade-off against higher power consumption.

2.3 Thermal Drift of Different Fluid-Filled Convective Accelerometer

Thermal drift, one disadvantage of microthermal accelerometer, is the change of sensitivity when the ambient temperature changes. Based on Equation (2.3), the sensitivity of convective accelerometer seems independent of the ambient temperature T_o. However, the thermophysical properties of working fluids are influenced by the ambient temperature. By analyzing the physical properties of working fluids and calculating their Rayleigh number, the main reason for thermal drift are discovered and a few solutions are proposed to reduce or eliminate the thermal drift. Also, the temperature-dependent response time of convective accelerometer using different working fluids is documented.

The physical properties of selected working fluids at the defined temperature range are documented in Table 2.4 [29, 30, 31, 32]. The response time and maximum differential temperature of different working fluid-filled convective accelerometer are calculated and listed in Table 2.5.

2.3.1 Gaseous Working Fluid

Although higher sensitivity can be achieved by selecting SF_6 or CO_2 as the working fluid, air is the most common working fluid for the convection-based microthermal accelerometer. The fluid's diffusivity plays an important role to determine the response time of convective accelerometers. The fluid's diffusivity can be calculated by Equation (2.10).

$$\alpha = \frac{k}{\rho c} \tag{2.10}$$

At the defined temperature range, the diffusivity of air is calculated to deduce its response time change. Also, the Rayleigh number of air is calculated and its MDT at different temperature are listed in Table 2.5. (Note that R.T. and MDT in this table and later on stand for the Response Time and Maximum Differential Temperature of convective accelerometer, respectively.)

The response time and MDT of air-filled convective accelerometer, which are calculated at different temperatures, are plotted to display the sensitivity change and response time change in Table 2.2. These two figures indicate that the sensitivity and response time of air-filled convective accelerometer become smaller when ambient temperature goes up. Note that the sensitivity of air-filled convective accelerometer at 273 K is almost 3 times the sensitivity at 353 K. To the convective accelerometer filled with intermediate-Prandtl-number working fluid, a few general conclusions are drawn:

- The sensitivities of convective accelerometer filled with gaseous working fluids are generally lower than that of convective accelerometer filled with liquid working fluids.

- The sensitivity of convective accelerometer filled with gaseous working fluid goes down when ambient temperature goes up.

- Empirical Equation (2.7) indicates that accelerometer response time is inversely proportional to the working fluid's diffusivity. Air's diffusivity at the defined temperature

Table 2.4: Physical Properties of Selected Working Fluids at Defined Temperature Range

Air					
T (K)	C $(J/Kg.K)$	ρ (Kg/m^3)	β (K^{-1})	μ $(Pa.s)$	k $(W/m.K)$
273	1004.9	1.2895	3.32e-3	1.7098e-5	0.0242
293	1006.5	1.2273	3.09e-3	1.8016e-5	0.0256
313	1008.0	1.1651	2.90e-3	1.8934e-5	0.0271
333	1009.6	1.1029	2.72e-3	1.9852e-5	0.0286
353	1011.2	1.0407	2.57e-3	2.0770e-5	0.0301
Isopropanol					
273	2267	801.4	1.12e-3	4.619e-3	0.141
293	2533	785.5	1.12e-3	2.396e-3	0.136
313	2617	768.4	1.12e-3	1.308e-3	0.132
333	2750	749.7	1.12e-3	0.837e-3	0.127
353	2883	732.9	1.12e-3	0.464e-3	0.123
DI Water					
273	4218	1002	0.18e-3	1.787e-3	0.552
293	4182	1000	0.18e-3	1.002e-3	0.597
313	4178	995	0.18e-3	0.653e-3	0.628
333	4184	985	0.18e-3	0.467e-3	0.651
353	4196	974	0.18e-3	0.355e-3	0.668
Ethylene Glycol					
273	2,294	1,131	0.65e-3	65.1e-3	0.242
293	2,382	1,117	0.65e-3	21.4e-3	0.249
313	2,474	1,101	0.65e-3	9.57e-3	0.256
333	2,562	1,088	0.65e-3	5.17e-3	0.260
353	2,650	1,078	0.65e-3	3.21e-3	0.261
Glycerin					
273	2,261	1,276	0.50e-3	10.604	0.281
293	2,386	1,264	0.50e-3	1.492	0.284
313	2,512	1,252	0.50e-3	0.275	0.287
333	2,637	1,236	0.50e-3	0.072	0.290
353	2,763	1,222	0.50e-3	0.0322	0.293
Methanol					
273	2,363	810	1.12e-3	0.8214e-3	0.210
293	2,406	791	1.12e-3	0.5850e-3	0.204
313	2,599	776	1.12e-3	0.4434e-3	0.199
333	2,940	753	1.12e-3	0.3722e-3	0.193
353	n/a	n/a	n/a	n/a	n/a

Table 2.5: Calculated Response Time and MDT of Selected Working Fluids at Defined Temperature Range

Air					
T(K)	$\alpha(m^2/s)$	Prandtl	R.T.(s)	Rayleigh	MDT(K)
273	0.18e-4	0.7100	0.707e-2	13.2e-4	3.8126e-3
293	0.21e-4	0.7083	0.634e-2	9.96e-4	2.8768e-3
313	0.24e-4	0.7043	0.580e-2	7.59e-4	2.1923e-3
333	0.26e-4	0.7008	0.538e-2	5.77e-4	1.6666e-3
353	0.29e-4	0.6978	0.504e-2	4.42e-4	1.2767e-3
Isopropanol					
273	0.77e-7	74.2643	0.715	0.2454	0.7088
293	0.68e-7	44.6255	0.809	0.5264	1.5204
313	0.65e-7	25.9321	0.847	0.9823	2.8372
333	0.61e-7	18.1240	0.902	1.5960	4.6098
353	0.58e-7	10.8757	0.949	2.9782	8.6021
DI Water					
273	1.31e-7	13.6550	0.422	7.57e-2	0.2186
293	1.43e-7	7.0190	0.386	12.33e-2	0.3561
313	1.51e-7	4.3443	0.365	17.79e-2	0.5138
333	1.55e-7	3.0014	0.355	23.55e-2	0.6802
353	1.64e-7	2.2299	0.338	29.61e-2	0.8552
Ethylene Glycol					
273	9.3274e-8	617	0.591	1.19e-2	0.0344
293	9.3585e-8	205	0.589	3.56e-2	0.1028
313	9.3984e-8	92	0.586	7.81e-2	0.2256
333	9.3275e-8	51	0.591	14.4e-2	0.4159
353	9.1364e-8	33	0.603	23.5e-2	0.6788
Glycerin					
273	9.7399e-8	8.5323e4	0.564	0.61e-4	0.0002
293	9.4167e-8	1.2535e4	0.583	4.41e-4	0.0013
313	9.1255e-8	0.2407e4	0.602	24.5e-4	0.0071
333	8.8975e-8	0.0655e4	0.617	94.5e-4	0.0273
353	8.6779e-8	0.0304e4	0.633	214e-4	0.0618
Methanol					
273	10.972e-8	9.2427	0.500	0.9875	2.8523
293	10.719e-8	6.8996	0.512	1.3860	4.0033
313	9.8670e-8	5.7909	0.556	1.9488	5.6288
333	8.7180e-8	5.6698	0.630	2.5497	7.3644
353	n/a	n/a	n/a	n/a	n/a

(a) **Response Time** (b) **MDT**
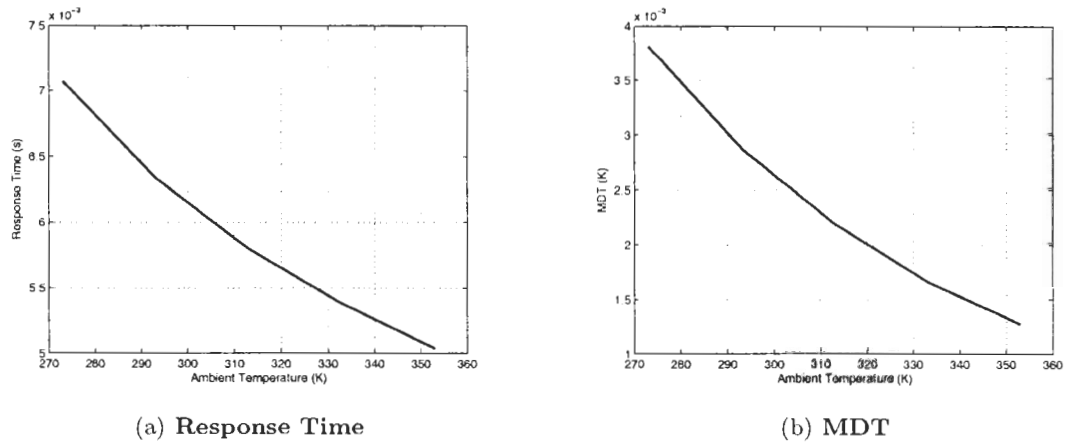
Figure 2.2: The Dimensional Analysis – Air

range goes up when ambient temperature goes up, hence the decreased response time of air-filled convective accelerometer.

- The calculated response times in Table 2.5 indicate that the response time of convective accelerometer filled with gaseous working fluids are significantly faster than those of convective accelerometer filled with liquid working fluids.

2.3.2 Liquid Working Fluids

The response time and MDT of DI water-filled convective accelerometer are plotted in Figure 2.3 to display the response time and sensitivity change. The results show that the sensitivity of the convective accelerometer using DI water as the working fluid goes higher when the ambient temperature goes up; the sensitivity of DI water-filled convective accelerometer at 353 K is about 4 times the sensitivity at 273 K. The calculated results also indicate that the response time decrease when the ambient temperature goes up. For a high-Prandtl-number fluid-filled convective accelerometer, say DI water, empirical Equation (2.8) indicates that response time is inversely proportional to the working fluid's diffusivity.

The results indicate that the sensitivity of ethylene glycol-filled convective accelerometer at 353 K is about 20 times the sensitivity at 273 K. The great sensitivity change can be explained by the temperature-sensitive dynamic viscosity of ethylene glycol. One interesting

(a) **Response Time**

(b) **MDT**
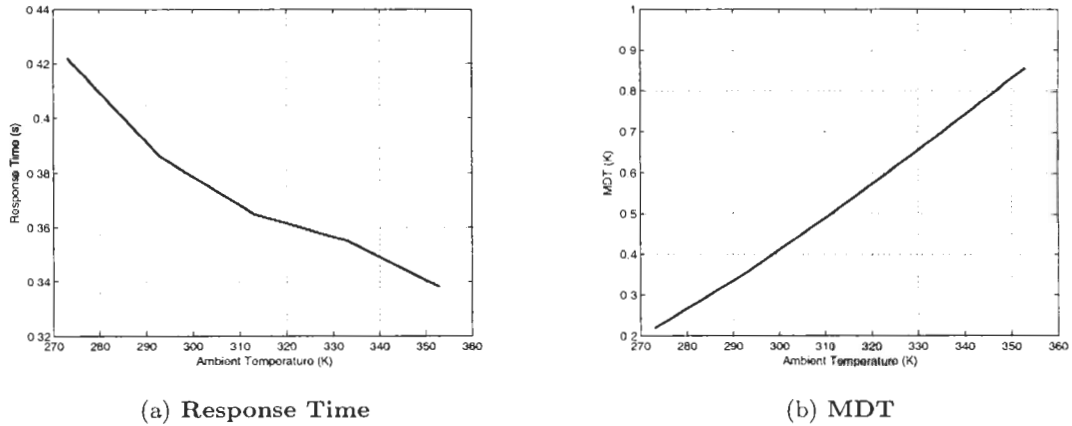
Figure 2.3: The Dimensional Analysis – DI Water

observation is that the response time of convective accelerometer filled with ethylene glycol is fluctuating slightly when ambient temperature goes up.

The calculated Rayleigh number indicates that the sensitivity of glycerin-filled convective accelerometer at 353 K is about 350 times the sensitivity of 273 K. The response time is very long at room temperature, but drops very rapidly when ambient temperature goes up. Among all the selected working fluids, the glycerin-filled convective accelerometer has the worst performance we ever researched.

The results indicate that the sensitivity of isopropanol-filled convective accelerometer at 353 K is about 12 times its sensitivity at 273 K. The response time increases when ambient temperature goes up.

Some prior literature [8] shows that the performance of liquid-filled convective accelerometer becomes unstable when the heater temperature is higher than working liquid's boiling point. Since the boiling point of methanol is 337.8 K, the physical properties of methanol at the temperature over its boiling point is not available. The results show that the sensitivity of methanol-filled convective accelerometer at 333 K is about 3 times the sensitivity at 273 K. Its response time increases when ambient temperature goes up.

2.4 Thermal Drift Analysis

The above theoretical calculations indicate that temperature dependence of Rayleigh number leads to convective accelerometers' sensitivity drift, whereas the temperature dependence of thermal diffusivity and Prandtl number lead to convective accelerometers' response time drift. The response times of different working-fluid-filled convective accelerometers were calculated over a defined temperature range. A few observations about the response time of convective accelerometer can be achieved from Lin's research [8]:

- The response time of gas-filled convective accelerometer is much faster than that of any liquid-filled convective accelerometer.

- To the convective accelerometer filled with intermediate or high-Prandtl-number working fluids, its response time is inversely proportional to the working fluid's diffusivity.

- To the convective accelerometer filled with low-Prandtl-number working fluids, its response time is inversely proportional to the product of Prandtl number and fluid's diffusivity, i.e., the ratio of fluid's dynamic viscosity to its density.

- In general, the thermal drift in response time is relatively insignificantly compared with the drift in sensitivity.

A few conclusions about the sensitivity and thermal drift were drawn by calculating Rayleigh number and MDT for different working fluid-filled convective accelerometers.

- The sensitivity of gas-filled convective microthermal accelerometer goes down when ambient temperature goes up.

- The sensitivity of liquid-filled convective microthermal accelerometer goes up when ambient temperature goes up.

- The sensitivity of convective accelerometer can be greatly improved by selecting liquid working fluids.

2.4.1 Steam as the Working Fluid

Considering steam is a vapor rather a gas, it was proposed to use vapor as the working fluid for convective accelerometer to reduce the thermal drift. The physical properties of steam

are listed in Table 2.6. An obvious drawback of using steam as the working fluid is that the heater temperature must be over 380 K so that steam can keep its gas state. Hence, the power consumption for steam-filled convective accelerometer would be higher than that of other gas-filled convective accelerometers. However, if the performance of steam appealed

Table 2.6: Physical Properties of Steam at Defined Temperature Range

$T(K)$	$C_p(J/Kg.K)$	$\rho\ (Kg/m^3)$	$\beta\ (K^{-1})$	$\mu(Kg/m.s)$	$k(W/m.K)$
380	2,060	0.5863	3.32e-3	12.71e-6	0.0246
400	2,014	0.5542	3.09e-3	13.44e-6	0.0261
450	1,980	0.4902	2.90e-3	15.25e-6	0.0299
500	1,985	0.4405	2.72e-3	17.04e-6	0.0339
550	1,997	0.4005	2.57e-3	18.84e-6	0.0379

sufficiently encouraging, it would be worthwhile to investigate other low-temperature vapors. The Prandtl and Rayleigh number are calculated and listed in Table 2.7.

Table 2.7: Calculated Prandtl Number and Rayleigh Number – Steam

T(K)	$\alpha(m^2/s)$	Prandtl	R.T.(s)	Rayleigh	MDT(K)
380	2.0368e-5	1.0643	0.0064	7.3687e-4	0.0021
400	2.3384e-5	1.0371	0.0058	5.3400e-4	0.0015
450	3.0806e-5	1.0099	0.0049	2.9655e-4	0.0009
500	3.8770e-5	0.9978	0.0043	1.7774e-4	0.0005
550	4.7387e-5	0.9927	0.0039	1.1299e-4	0.0003

The sensitivity and response time change for steam-filled convective accelerometer are plotted in Figure 2.4. The results indicate that the sensitivity of steam-filled convective accelerometer falls when ambient temperature goes up, and the sensitivity at 380 K is about 6 times the sensitivity at 550 K.

The above theoretical calculations suggest that steam is not the working fluid we are looking for to reduce thermal drift. And, power consumption for steam-filled convective accelerometer is higher than most liquid-filled convective accelerometers. The definition of Rayleigh

(a) **Response Time**   (b) **MDT**
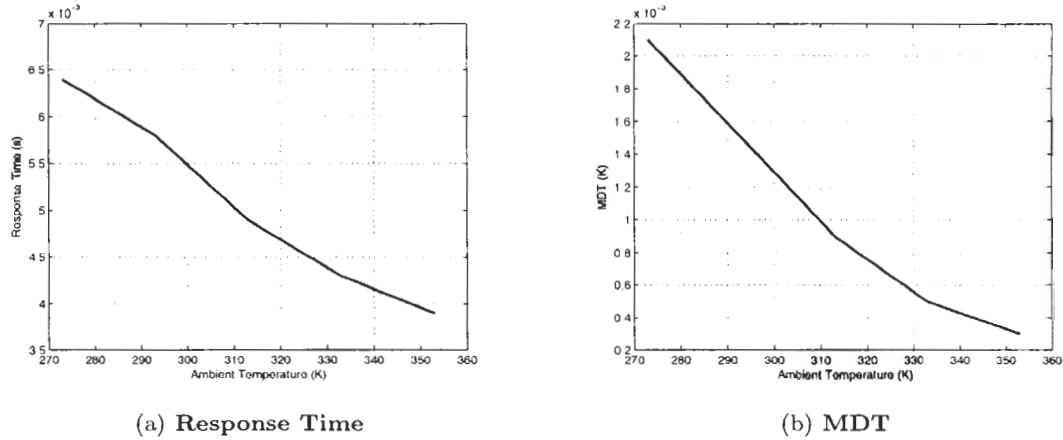
Figure 2.4: The Dimensional Analysis – Steam

number and the physical properties of working fluids give us a challenge: find one ideal working fluid so that the Rayleigh number at the defined temperature range keeps approximately constant when ambient temperature changes.

2.4.2   Mercury as the Working Fluid

One important observation comes from analyzing the working fluids' temperature-dependent physical properties. In the liquid-filled convective accelerometer, the *dynamic viscosity* of all liquids becomes smaller when ambient temperature goes up, and this is the dominant factor causing the Rayleigh number of working fluids to become bigger. In the gas-filled convective accelerometer, although the dynamic viscosity of all gases also becomes bigger when ambient temperature goes up, which *does* contribute to a part of Rayleigh number change, the main reason is that the *density* of gas becomes lower as the ambient temperature increases, which contributes most of the change in Rayleigh number.

To select an ideal working fluid to reduce or eliminate the thermal drift of convective accelerometer, the viscosity temperature coefficient of fluids is introduced. The coefficient is defined by Equation (2.11).

$$\zeta = \frac{\mu_{40} - \mu_{100}}{\mu_{40}} \tag{2.11}$$

where: μ_{40} and μ_{40} stand for the dynamic viscosity of fluid at 40 °C and 100 °C, respectively. The coefficient will be negative for many gases, but positive for many liquids. The

ideal liquid for minimizing thermal drift would have a viscosity temperature coefficient of 0.

By carefully searching dozens of working fluids, mercury is selected as a candidate for convection-based microthermal accelerometer. The research results show that dynamic viscosity of mercury does not change too much at defined temperature range. The physical properties of mercury at different temperatures, from 273 K to 353 K, are listed in Table 2.8.

Table 2.8: Physical Properties of Mercury At Defined Temperature Range

$T(K)$	$C_v(J/Kg.K)$	$\rho\ (Kg/m^3)$	$\beta\ (K^{-1})$	$\mu(Kg/m.s)$	$k(W/m.K)$
273	140.3	13,628	1.82e-4	1.69e-3	8.20
293	139.4	13,579	1.82e-4	1.55e-3	8.69
313	138.6	13,506	1.82e-4	1.40e-3	9.40
333	137.3	13,385	1.82e-4	1.24e-3	10.5
353	136.5	13,264	1.82e-4	1.13e-3	11.5

At defined temperature range, the calculated response time and MDT of convective accelerometer filled with mercury are listed in Table 2.9. The calculated Rayleigh number at different temperatures suggests that the sensitivity of mercury-filled convective accelerometer probably does not change much. This prediction will be confirmed by conducting numerical simulations in next chapter. The theoretical calculations also indicate that the

Table 2.9: Calculated Prandtl Number and Rayleigh Number – Mercury

T(K)	$\alpha(m^2/s)$	**Prandtl**	**R.T.(s)**	**Rayleigh**	**MDT(K)**
273	42.9e-7	0.0289	0.162	3.35e-2	0.0968
293	46.1e-7	0.0249	0.176	3.40e-2	0.0982
313	48.7e-7	0.0206	0.200	3.43e-2	0.0991
333	51.5e-7	0.0162	0.241	3.37e-2	0.0973
353	54.2e-7	0.0134	0.276	3.30e-2	0.0953

response time of mercury-filled convective accelerometer increases slightly when ambient temperature goes up.

For comparison, a few working fluids, including air, DI water, isopropanol, methanol, and mercury, are selected and their calculated Rayleigh number are normalized at 293 K. The
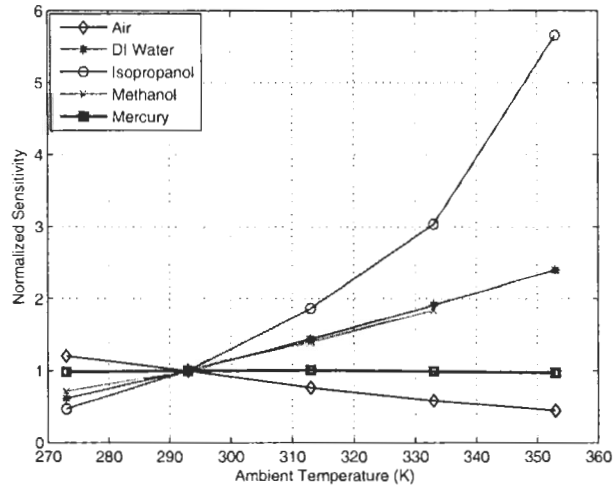
Figure 2.5: Relative Sensitivity Drifts, normalized at 293 K

normalized Rayleigh numbers are plotted in Figure 2.5. The normalized results indicate that mercury-filled convective accelerometer can achieve the least sensitivity drift; isopropanol-filled convective accelerometer has the most sensitivity drift among all selected working fluids.

Their theoretical response time are normalized at 293 K and plotted in Figure 2.6. The normalized results indicate that ethylene glycol-filled convective accelerometer can achieve the least response time drift, although the size of this drift is relatively small for all fluids studied.

2.5 Conclusions

In this chapter, the convection-based microthermal accelerometer was modeled as an infinitely long, horizontal, pair of concentric cylinders. Hodnett's solution shows that the sensitivity of convection-based microthermal accelerometer is proportional to Rayleigh number. A few methods can be employed to improve the sensitivity of convective accelerometer. A few fluids were selected as potential working fluids for convective accelerometer and their
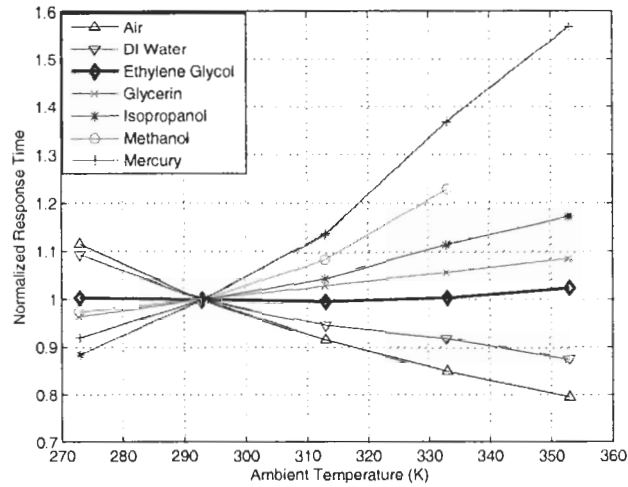
Figure 2.6: Relative Response Time Drifts, normalized at 293 K

physical properties at the defined temperature range are documented.

By analyzing the change of Rayleigh number at different temperatures, the main reasons which lead to the thermal drift of convection-based micromachined accelerometer are discovered. Some important conclusions can be drawn.

- The sensitivity of convective accelerometer was improved two or three orders of magnitude when liquid was selected as the working fluid instead of a gas.

- The sensitivity of gas-filled convective accelerometer decreases when ambient temperature goes up; in contrast, the sensitivity of liquid-filled convective accelerometer increases when ambient temperature goes up.

- Both air-filled and liquid-filled convective accelerometer suffer from thermal drift.

Steam and mercury are selected as candidate working fluids to reduce this drift. The theoretical calculation for steam-filled convective accelerometer shows that the thermal drift still exist. Comparing to other selected working fluid, the calculation of Rayleigh number for mercury-filled convective accelerometer suggest that its drift is almost zero. This prediction will be further confirmed by conducting some numerical simulations in ANSYS.

Based on prior literature, the response times of convective accelerometers filled with different working fluids are calculated. The variations in response time are relatively small in comparison to the variations in sensitivity.

Chapter 3

Convective Accelerometer – Numerical Simulation

In this chapter, a FLOTRAN model of convection-based microthermal accelerometers, a pair of concentric cylinders, is constructed for numerical simulations. During the numerical simulation study, the polysilicon heater was modeled either as a constant heat flux heater or constant differential temperature heater. For the convective accelerometer filled with gaseous working fluids, the simulations are conducted under one of two assumptions: constant volume condition or constant pressure condition. This allows us to investigate some details which were not represented in Hodnett's model.

One important concept, the position where Maximum Differential Temperature occurs, or 'MDT', is analyzed. Using different meshing sizes, the location and magnitude of MDT are founded for the convection-based micromachined accelerometer. The performance of the convective accelerometer filled with selected working fluids is documented, and the thermal drift of the convective accelerometer is eliminated by using mercury as the working fluid.

3.1 FLOTRAN Model

The FLOTRAN model of the convective accelerometer is shown in Figure 2.1. Hodnett used the same model and solved the governing equations. The inner and outer cylinder stand for the polysilicon heater and cavity of the convective accelerometer, respectively.

In this model, the temperature sensors are not represented; instead, the best location of temperature sensors, which is the position where MDT occurs, will be deduced from the simulation results. The complete simulation procedures for building models and setting parameters are described in Appendix II.

3.1.1 Meshing
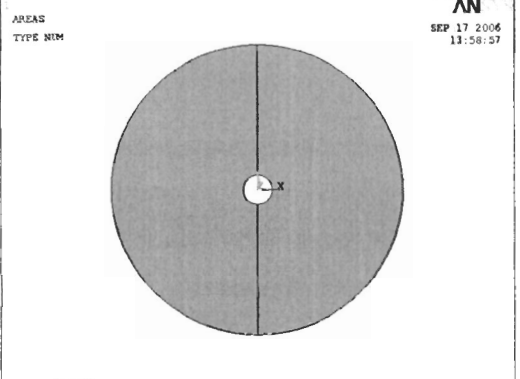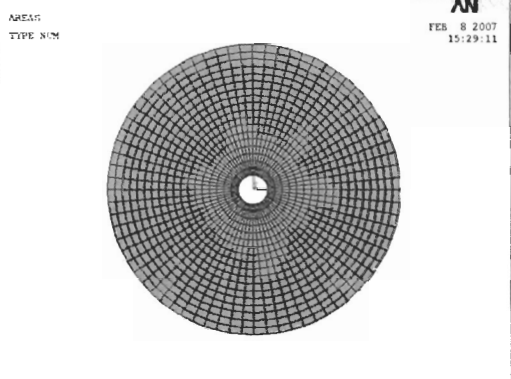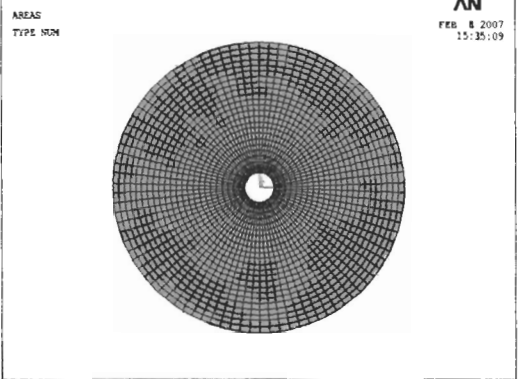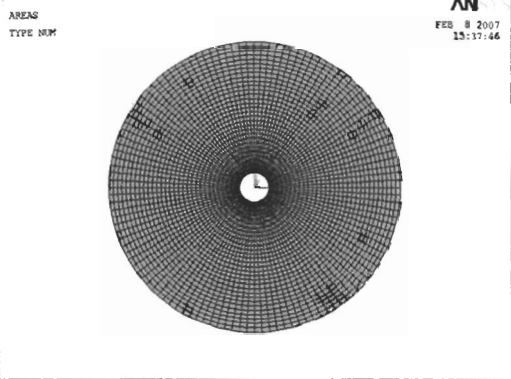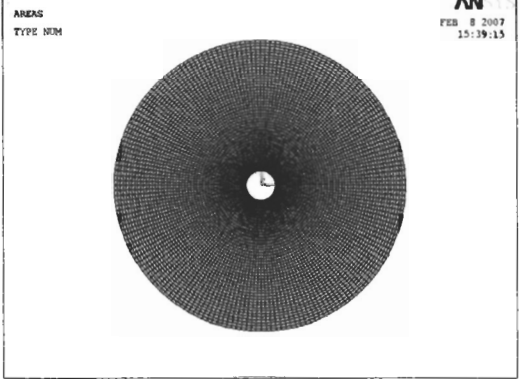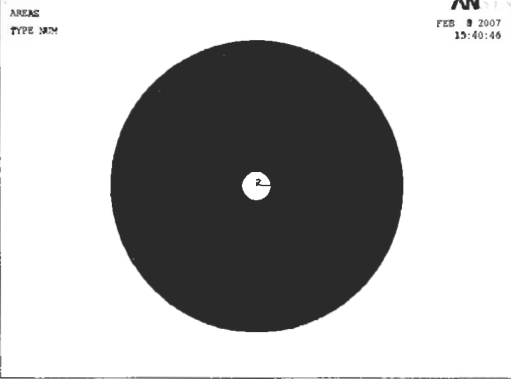
The FLOTRAN model can be automatically meshed in ANSYS. To achieve more accurate results, better control over the meshing method for the FLOTRAN model can be achieved by manually defining the sizes of elements in the radial and circumferential directions. In this case, the left half side of concentric cylinder is constructed and meshed, then the concentric cylinder is completed by reflecting the left half side to the right half side. Based on the theory of finite element analysis, the more fine elements are defined in the model, the more accurate result can be achieved. Two methods are used to improve the meshing performance for the FLOTRAN model of convection-based microthermal accelerometers.

Method 1: Refine Meshing Size

As mentioned early, the smaller size elements that are defined, the more accurate result can be achieved by the model. However, the cost of very fine element size is longer computing time. To make sure reasonable sized elements had been chosen, various sizes of elements, ranging from 50 μm and 5 degrees to 10 μm and 1 degree in the radial and circumferential directions respectively, are defined in the FLOTRAN model. The meshed models with different meshing sizes are listed in Table 3.1.

The numerical simulations for different meshing sizes were conducted for the air-filled convective accelerometer. It took around 15 minutes in a SUN workstation (SunBlade 1500) to finish the simulation with the coarsest meshing, 50 μm and 5 degrees in the radial and circumferential direction, respectively. Not too much valuable information could be achieved from these simulation results. On the other hand, it took the same SUN workstation over 10 hours to finish the simulation with the finest meshing, 10 μm and 1 degree in the radial and circumferential direction, respectively. The meaningless former simulation results and the computing time for the later simulation encouraged us to find a more reasonable meshing size for this FLOTRAN model.

Table 3.1: The Meshed Model at Different Element Size

(a) **Standard Mesh**   (b) **Refined Mesh**

Figure 3.1: The Standard Meshed Model and Refined Model

Method 2: Define Space Ratio

Uniform meshing is first applied to the FLOTRAN model and is shown in the left figure of Figure 3.1. Note that the elements near the outer cylinder are wide, flat bricks, while those near the inner cylinder are tall, narrow bricks. The model can be refined by defining the space ratio parameter. This parameter sets the ratio of the radial extent of the elements at minimum radius to their radial extent at maximum radius. In this model, it is set equal to the ratio of the radius of outer cylinder to the radius of inner cylinder. Hence, the radial meshing size of elements around the inner cylinder is 10 times smaller than that of elements around the outer cylinder. The FLOTRAN model is refined and shown in the right figure of Table 3.1. Note that all the elements are now approximately squares.

3.1.2   The Definition of MDT

In this work, MDT stands for the Maximum Differential Temperature of convection-based microthermal accelerometer. The two temperature sensors are located in the position where MDT occurs so that high sensitivity is achieved. Based on Hodnett's solution, the position of MDT can be deduced from Equation (2.1). It tells us where the temperature sensors should be located. In this section, simulations using different meshing size are conducted to confirm the position and magnitude of MDT.

Table 3.2: Simulation Results for Air-filled Convective Accelerometer

Meshing Size	Nodes	Location(μm)	MDT (K)
50 μm, 5°	1406	415	0.00277195
40 μm, 4°	2208	413	0.00279408
30 μm, 3°	3782	400	0.00281776
20 μm, 2°	8372	400	0.00282933
10 μm, 1°	32942	400	0.00282721

The simulation results indicate that the position of MDT is about one third of the distance from the inner cylinder across the annulus to the outer cylinder. Also, the position of MDT is independent of selected working fluids, which means the original air-filled convective accelerometer can be used as the convective accelerometer using other liquid working fluids.

A few assumptions are made before the numerical simulations:

- To the polysilicon heater, radiative heat transfer is negligible.

- All the selected working fluids are laminar and incompressible.

- No heat source within the cylindrical annulus.

Air is selected as the working fluid to determine the MDT of convective accelerometer. The simulation results are listed in Table 3.2. The simulation results show that the position of MDT approaches a limiting value when finer meshing sizes are defined. The magnitude of MDT deduced from different meshing sizes is plotted in Figure 3.2. An important conclusion is that the meshing sizes of element, 30 μm and 3 degrees in the radial and circumferential direction, are fine enough to achieve accurate results.

The positions and magnitudes of MDT using different meshing size are plotted in Figure 3.3. The simulation results indicate the position of MDT is located at a radius of 400 μm.
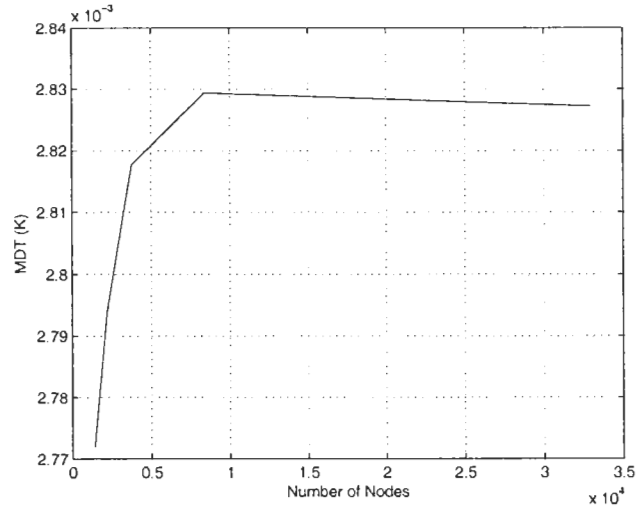
Figure 3.2: The Magnitude of MDT Deduced from Different Meshing Sizes
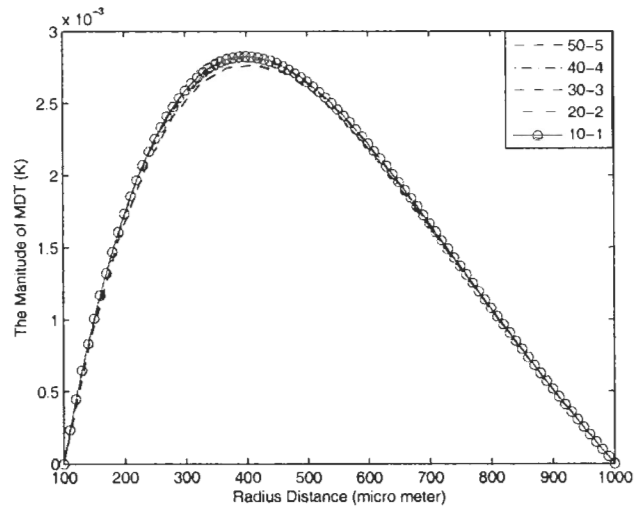
Figure 3.3: The Positions and Magnitude of MDT Using Different Meshing Size

3.2 Convection-Based Micromachined Accelerometer Without Temperature Sensors

In this section, a variant on the convective accelerometer is described. In the original design, two temperature sensors located in the position where maximum differential temperature occurs detect the differential temperature and the applied acceleration is deduced from the signal output. Based on the variation of electrical resistance with temperature, a temperature-sensitive resistor can be used as a temperature sensor and a heater. The applied acceleration can then be deduced from the electrical resistance change of this polysilicon heater, and the two sensors eliminated.

This innovative idea motivates another new concept – the Convection-Based Accelerometer Without Temperature Sensors. In this design, the two temperature sensors are removed from the original convection-based micromachined accelerometer. Some prior literature indicates [8] that the resistance of polysilicon heater linearly increases when its temperature goes up, so the heater in this design is also a temperature sensor. Heat is transferred from the polysilicon heater to the surrounding medium, and the rate of heat transfer increases with natural convection.

3.2.1 The Design Principle

The convective accelerometer without thermopiles is a variant of the convection-based micromachined accelerometer requiring no thermopiles in the design. A few milli-amps current are passed through the heater and a symmetric temperature distribution is generated around the heater when no acceleration is applied to the accelerometer. The symmetric temperature distribution is disturbed by the buoyancy force due to the applied acceleration. Some heat is taken away from the heater, which causes a temperature drop. If polysilicon is used as the heater material, the electrical resistance will decrease after the applied acceleration. The acceleration can in principle be deduced from the resistance change of the heater.

3.2.2 Numerical Simulations

A FLOTRAN model of the convection-based microthermal accelerometer was created. Air was selected as the working fluid and the heater was controlled as a constant-flux heater. A

Table 3.3: Simulation Results for the Convective Accelerometer Without Temperature Sensors

$T(K)$	$T_i(K)$	$T_a(K)$	$\triangle T(K)$	$MDT(K)$
273	282.3836051	282.3836035	0.0000016	0.0046205
293	301.8162545	301.8162538	0.0000007	0.0033950
313	321.3268082	321.3268079	0.0000003	0.0025557
333	341.8981113	340.8981111	0.0000002	0.0019627
353	360.5195016	360.5195015	0.0000001	0.0015340

standard gravitational acceleration was applied to the accelerometer. Simulations were conducted and results analyzed to predict the performance of convective accelerometer without temperature sensors.

The simulation results are shown in Table 3.3. T_i and T_a in the table stand for the temperature of polysilicon heater before and after the acceleration is applied, respectively. The acceleration can be deduced from the temperature change of heater, $\triangle T$. The simulation results of heater-temperature accelerometer were compared with the MDT of original convection-based microthermal accelerometer in Table 3.3. We note that the modified design has a sensitivity about four orders of magnitudes lower than the original, and that this sensitivity decreases rapidly as ambient temperature increase.

Although the temperature of the heater does change in response to acceleration, the sensitivity of this design is much lower than that of the original convection-based micromachined accelerometer with thermopiles. Moreover, this design variant is at least as susceptible to thermal drift as the original design.

3.3 The Performance of Selected Working Fluids

To investigate the sensitivity improvement and thermal drift of the convection-based micromachined accelerometer, a few working fluids, including air and some liquids, are selected as potential working fluids to test their performance. In chapter 2: Convective Accelerometer – Dimensional Analysis, the solution of the governing equations shows that the sensitivity of convective accelerometer is proportional to the Rayleigh number. Based on the definition

of Rayleigh number, one effective method is to use working fluids with higher density, such as liquids, to improve the sensitivity of convective accelerometer. The previous theoretical calculations also suggest that acceptable thermal drift of convective accelerometer could be achieved by using mercury as the working fluid.

3.3.1   Two Different Types of Heating Element Control

The thermal conductivity of working fluids is a temperature-dependent parameter and so when the ambient temperature changes, we can choose either to keep heat flux constant or the temperature difference between cylinders, $\triangle T$, constant. To discover the performance change of convective accelerometer, the inner cylinder is modeled either as a constant heat flux surface or constant differential temperature heater.

In the case of constant differential temperature between the inner and outer cylinders, the heater is modeled as 10 K higher than the temperature of outer cylinder.

In practice it may be simpler to keep the heat flux constant. We assume a constant electrical current through the polysilicon heater. To compare the simulation results with the case of constant differential temperature, the heat flux is calculated so that at an ambient temperature 273 K the temperature of inner cylinder is 10 K higher than that of outer cylinder. The heat flux is then maintained constant as ambient temperature changes. If the thermal conductivity of working fluid goes up when ambient temperature goes up, the temperature difference between the cylinders will go down.

Equation (3.1) and Equation (3.2) are used to calculate corresponding heat flux for different working fluids.

$$T_i - T_o = Q \frac{\ln(r_o/r_i)}{2\pi kl} \tag{3.1}$$

$$q = \frac{Q}{A} \tag{3.2}$$

Where:

T_i, T_o: the temperature of inner and outer cylinder, respectively (K)

r_i, r_o: the radius of inner and outer cylinder, respectively (m)

k: the thermal conductivity of working fluid $(W/m.K)$

l: characteristic length of heater (m)

Q: the power passed through the polysilicon heater (W)

A: the area of heating element (m^2)

3.3.2 Gas-Filled Convective Accelerometer

Air as the Working Fluid

There are a few gases can be selected as potential working fluids for the convection-based micromachined accelerometer. Due to its low cost and ready availability, air is the original working fluid for the convective accelerometer. There are many advantages to the air-filled convective accelerometer. We can seal the accelerometer chip using TO-8 packing in the ambient environment. More important, air is non-corrosive to the physical structure of microthermal accelerometer in the long run.

Two sets of boundary conditions are considered in modeling the air-filled convective accelerometer. One case is assuming the inner pressure of cavity keeps constant, i.e., the pressure of cavity does not change when the ambient temperature changes. The other case is assuming the inner volume of cavity keeps constant, i.e., the volume of cavity is tightly sealed as ambient temperature changes.

The simulation results for the case in which the heater is controlled as a constant heat flux heater are listed in Table 3.4. The thermal drift for different boundary condition is plotted in Figure 3.4. Two observations can be made from these simulation results:

- For the air-filled convective accelerometer, the sensitivities in both cases (Constant Volume and Constant Pressure) go down when ambient temperature goes up.

- The thermal drift in the constant volume case is better than the thermal drift in the constant pressure case.

For comparison, the simulation results for the case in which the heater is controlled at constant differential temperature are listed in Table 3.5. The thermal drift for both cases is plotted in Figure 3.5. Two similar conclusions can be drawn from the above simulation results.

Table 3.4: Simulation Results of Air-Filled Convective Accelerometer (Constant Heat Flux)

Ambient Temperature (K)	Constant Volume (K)	Constant Pressure (K)
273	0.0046205	0.0046205
293	0.0033950	0.0029474
313	0.0025557	0.0019442
333	0.0019627	0.0013191
353	0.0015340	0.0009175
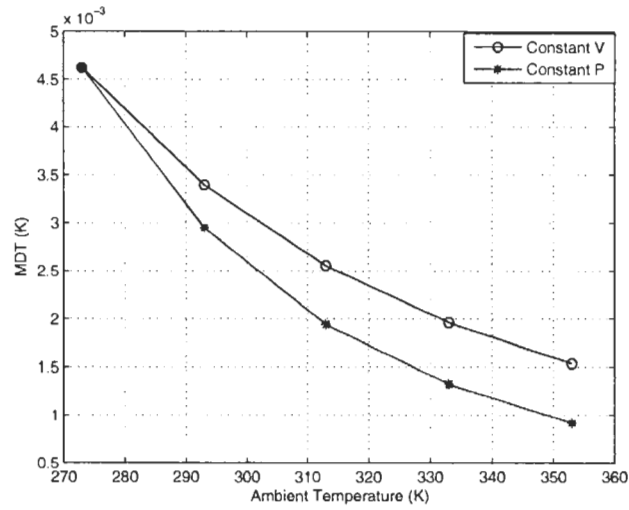
Figure 3.4: Thermal Drift of Air-Filled Convective Accelerometer in Two Boundary Conditions (Constant Heat Flux)

Table 3.5: Thermal Drift of Air-Filled Convective Accelerometer (Constant Differential Temperature)

Ambient Temperature (K)	Constant Pressure (K)	Constant Volume (K)
273	0.00424644	0.00424644
293	0.00306283	0.00352804
313	0.00226334	0.00297518
333	0.00170692	0.00253986
353	0.00131040	0.00219093
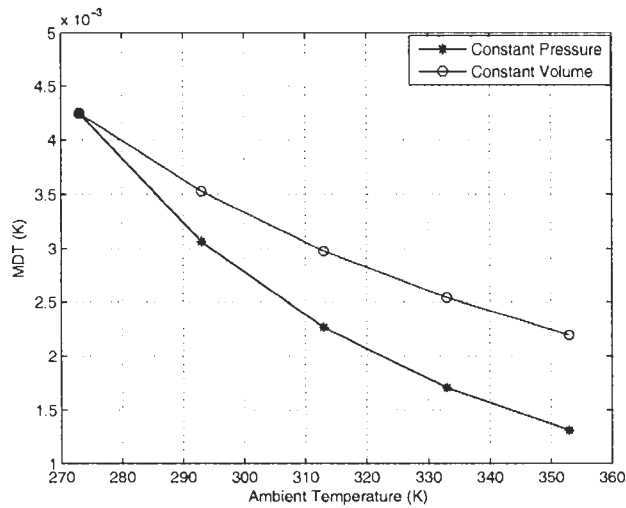
Figure 3.5: Thermal Drift of Air-Filled Convective Accelerometer in Two Boundary Conditions (Constant Differential Temperature)

The above simulations results suggest that the thermal drift of gas-filled convective accelerometer in the case of constant volume is always better than that in the case of constant pressure, which confirms that density change is a main factor responsible for the sensitivity change. Meanwhile, the simulation results for the constant differential temperature heater in the case of constant volume are compared to the simulation results for the constant heat flux heater in the case of constant volume. The results are shown in Figure 3.6. An important observation from Figure 3.6 is that the thermal drift of the air-filled microthermal accelerometer is better if the heater is controlled as a constant differential temperature heater.

3.3.3 Liquid-Filled Convective Accelerometer

Hodnett's solution indicates that the convective accelerometer chip using air as the working fluid may be used as an accelerometer using other kinds of liquids, since the position of maximum differential temperature is independent of different working fluids. Based on the Rayleigh number calculated in Chapter 2, the sensitivity of some working liquid, such as methanol, can be a few hundred times the sensitivity of air-filled convective accelerometer.

Two different series of simulations are conducted in which the heater is controlled as a
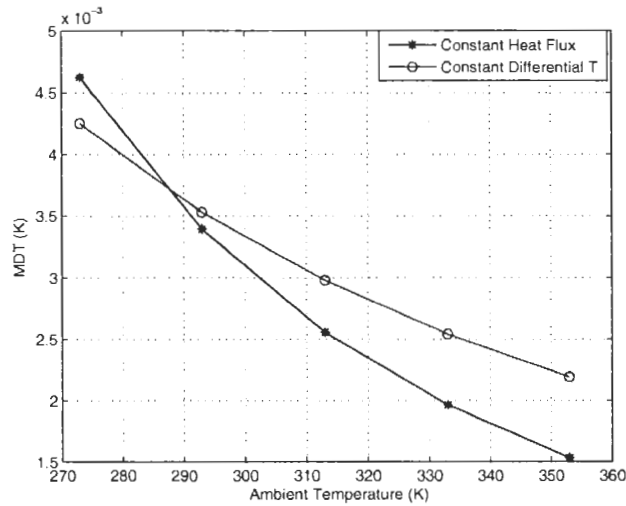
Figure 3.6: Simulation Results Comparison for Constant-Volume Air

constant differential temperature heater and a constant heat flux heater. The simulation results of DI water-filled microthermal accelerometer are plotted in Figure 3.7. In contrast to air, one conclusion for this case is that the thermal drift in the case of constant heat flux heater is better than that in the case of constant differential temperature heater. The simulation results agree with the previous theoretical calculations: the sensitivity of DI water-filled convective accelerometer at 353 K is around 4 times the sensitivity at 273 K.

The theoretical calculations in Chapter 2 indicate that the sensitivity of the isopropanol-filled convective accelerometer at 353 K is about 12 times its sensitivity at 273 K. Apparently, high sensitivity of convective accelerometer can be achieved by using isopropanol as the working fluid, but the cost is high thermal drift. Two different series of simulations are conducted in which the heater is controlled as a constant differential temperature heater and a constant heat flux heater. Although the ethylene-glycol-filled convective accelerometer has the least response time drift among the selected working fluids, glycol is not a suitable working fluid to reduce the sensitivity drift. The simulation is conducted only to test our prediction. The heater is controlled as a constant heat flux heater during the simulations. The simulation results show that the sensitivity of ethylene glycol-filled convective accelerometer at 353 K is around 18 times its sensitivity at 273 K, which followed the previous theoretical calculations.
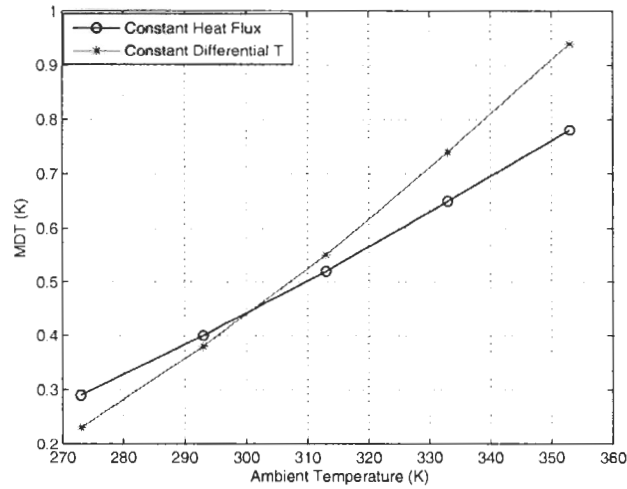
Figure 3.7: The MDT of DI Water-Filled Convective Accelerometer

Methanol might be a good working fluid for the convective accelerometer to reduce the sensitivity drift. Theoretical calculations for the methanol-filled convective accelerometer suggest that the sensitivity at 333 K is about 2.5 times the sensitivity at 273 K. The simulations are conducted for a methanol-filled convective accelerometer in which the heater is controlled as a constant-heat-flux heater. The sensitivity of methanol-filled convective accelerometer at 333 K is 1.37 times the sensitivity at 273 K. In some applications, this drift might be acceptable. In addition, the sensitivity of methanol-filled convective accelerometer is very high compared with all the other selected working fluids. However, one of its drawbacks is that its performance becomes unstable when the heater temperature is higher than methanol's boiling point 337.8 K. Another drawback is that methanol is an electrically-conductive liquid, which means it is not a suitable working fluid for the convection-based microthermal accelerometer.

Among all the selected working fluids, the theoretical calculations indicate that glycerin-filled convective accelerometer has the worst thermal drift. Chapter Two's analysis showed that the sensitivity of glycerin-filled convective accelerometer at 353 K is about 350 times the sensitivity at 273 K, which can be explained by its very temperature-sensitive dynamic

Table 3.6: Simulation Results for Steam-filled Convective Accelerometer

	273 K	**293 K**	**313 K**	**333 K**	**353 K**
$MDT_v(K)$	0.00206541	0.00151902	0.00078052	0.00044085	0.00026540
$MDT_p(K)$	0.00206541	0.00137093	0.00055657	0.00025464	0.00012675

viscosity. The simulation results show that the sensitivity of glycerin-filled convective accelerometer at 353 K is about 344 times of sensitivity at 273 K, very close to the previous theoretical calculations.

Although steam is a vapor rather than gas, the thermal drift of steam-filled convective accelerometer is still unacceptable high. The previous calculations suggest that the thermal drift of convective accelerometer could be eliminated by using mercury as the working fluid. For comparison, the conventional method to compensate the thermal drift of convective accelerometers is described.

The theoretical calculation for steam-filled convective accelerometer indicates that the sensitivity at 380 K is about 6 times the sensitivity at 550 K. Although the calculated results suggest that steam is not a suitable working fluid to reduce thermal drift, the simulation are still conducted to confirm our prediction.

The heater is controlled as a constant heat flux heater during the simulations. The simulation results are listed in Table 3.6. Note that in Table 3.6, MDT_v stands for the maximum differential temperature in the case of constant volume and MDT_p stands for the maximum differential temperature in the case of constant pressure.

The simulation results indicate that the thermal drift of steam-filled convective accelerometer is worse than the thermal drift of air-filled convective accelerometer. In addition, to generate and keep steam state, the power consumption would a few times greater than the air-filled microthermal accelerometer.

Table 3.7: Simulation Results for Mercury-filled Convective Accelerometer (Constant Heat Flux)

	273 K	**293 K**	**313 K**	**333 K**	**353 K**
$MDT(K)$	0.12307154	0.10910864	0.09394257	0.07696648	0.06612003

3.3.4 Mercury As the Working Fluid

The Rayleigh numbers of different working fluids calculated in Chapter 2 show that the thermal drift of the convective accelerometer results from some physical properties of the working fluids. The conventional solution [18] to eliminate thermal drift is to use an outside circuit to compensate this drift at different temperatures. After simulating a number of possible working fluids, our results indicate that both good sensitivity and acceptable thermal drift can be achieved if mercury is selected as the working fluid for a convective accelerometer.

The previous theoretical calculations indicate that the sensitivity of mercury-filled convective accelerometer does not change much over the defined temperature range. Two series of numerical simulations are conducted in which the heater is controlled as a constant heat flux heater and a constant differential temperature heater.

The simulation results are listed in Table 3.7, in which the heater is controlled as a constant heat flux heater. The results show that the sensitivity of mercury-filled convective accelerometer at 273 K is about twice the sensitivity at 353 K, which does not follow the previous theoretical calculations. So far, mercury is the only liquid working fluid which sensitivity goes down as ambient temperature goes up. For comparison with other liquids, a few possible choices, including air, isopropanol, DI water and mercury, are selected and their sensitivities normalized at 293 K. The normalized sensitivities are plotted in Figure 3.8.

The reason why the simulation results do not follow the previous theoretical calculation is mercury's temperature-sensitive thermal conductivity. The thermal conductivity of mercury goes up when ambient temperature goes up. Hence for constant heat flux the temperature
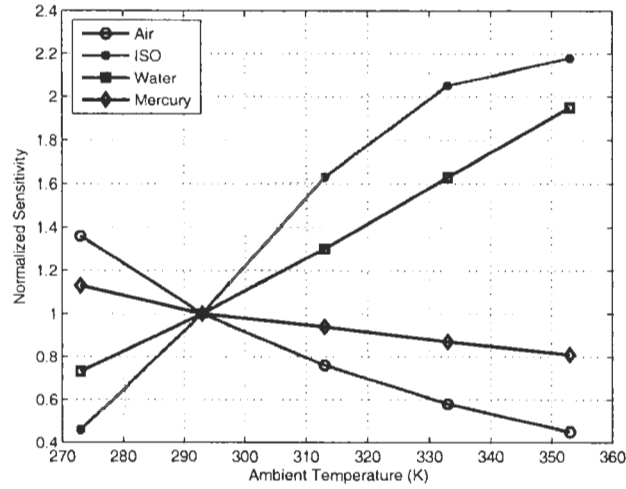
Figure 3.8: Relative Thermal Drifts (Constant Heat Flux), normalized at 293 K

Table 3.8: Simulation Results for Mercury-filled Convective Accelerometer (Constant Differential Temperature)

	273 K	**293 K**	**313 K**	**333 K**	**353 K**
$MDT(K)$	0.10266011	0.10298005	0.10372659	0.10436767	0.10481892

difference between the inner and outer cylinder goes down when ambient temperature goes up. To avoid this problem, the heater is controlled as a constant differential temperature heater. The simulation results are listed in Table 3.8. The sensitivity of the same four selected working fluids are normalized at 293 K and plotted in Figure 3.9.

3.4 Solutions to Eliminate Thermal Drift

3.4.1 Conventional Solution

One conventional solution [19] provided by MEMSIC Corp. is to use a built-in temperature sensor in the input network to compensate for the sensitivity drift. For the air-filled
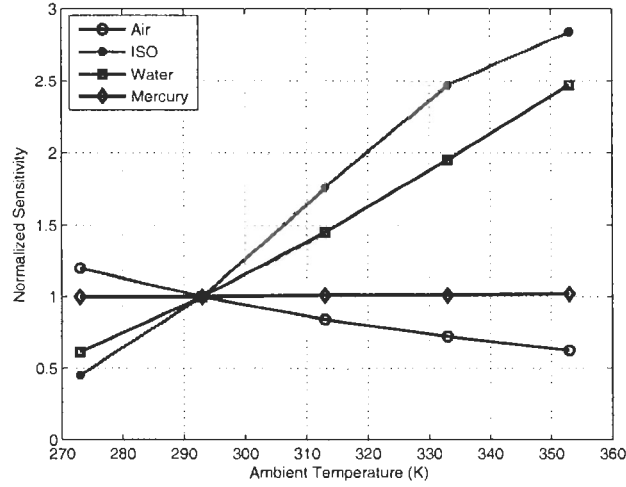
Figure 3.9: Relative Thermal Drifts (Constant Differential Temperature), normalized at 293 K

convection-based accelerometer, the sensitivity at an ambient temperature T_f can be deduced from Equation (3.3).

$$S_f = (\frac{T_i}{T_f})^{2.67} \cdot S_i \tag{3.3}$$

where:

S_f: the sensitivity at the final temperature ($\mu V/g$)

S_i: the sensitivity at the initial temperature ($\mu V/g$)

T_i, T_f: the initial and final temperatures, respectively (K)

For applications where sensitivity changes of a few percent are acceptable, Equation (3.3) can be approximated with a linear function. An external circuit that provides a gain adjustment of $0.9\%/°C$ would keep the sensitivity within 5% of its room temperature value [19]. To the applications that demand very low sensitivity change, a micro-controller can be used to compensate this drift. The compensation circuit is shown in Figure 3.10.

A NTC (Negative Temperature Coefficient) thermistor is selected in the compensation circuit. Based on different selected thermistors, the compensation performance is shown in Table 3.9. Relative low sensitivity drift of convective accelerometers using air as the working fluid can be obtained by selecting different thermistors in the compensation circuit.
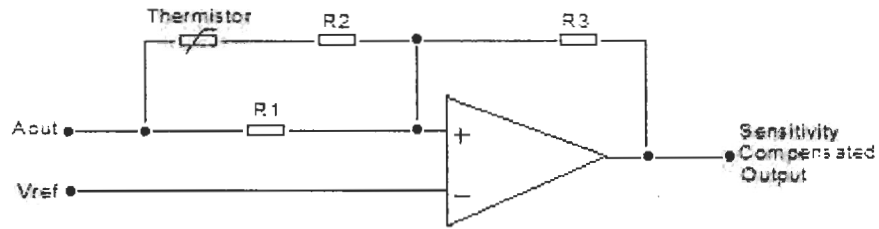
Figure 3.10: Thermistor-Controlled Gain Circuit

Table 3.9: Compensation Performance

R1(Ω)	R2(Ω)	R3(Ω)	Thermistor(Ω)	Sensitivity Error
12 k	4.3 k	4.7 k	5 k(Changzhou)	9%
20 k	10 k	10 k	10 k(Panasonic SMD)	13%
20 k	10 k	10 k	10 k(QTI or YSI curve Z)	14%

An instant drawback of the conventional solution is that the total cost of the convective accelerometer is increased. In addition, the selected thermistor and other electrical components themselves in the compensation circuit suffer from thermal drift as well, which make the thermal drift of convective accelerometers harder to predict. Therefore, the more complicated signal output process system, the higher possibility of system failure and cost.

3.4.2 Solution by Choice of Working Fluid

In chapter 2, a few theoretical calculations were performed for different working-fluid-filled convective accelerometers. The Rayleigh numbers are calculated and the main reasons which led to the thermal drift of convective accelerometer are discovered. A few important observations can be drawn from this comparison:

- Theoretical calculations and numerical simulation both indicate that the sensitivity of gas-filled convective accelerometer goes down when ambient temperature goes up; whereas the sensitivity of liquid-filled convective accelerometer goes up when ambient temperature goes up.

- The thermal drift of convection-based micromachined accelerometer can be perfectly eliminated by using mercury as the working fluid.

3.5 Conclusion

In this chapter, the convection-based micromachined accelerometer was modeled as a pair of concentric cylinders by using the CFD program 'FLOTRAN'. The definition of MDT was introduced, and the magnitude and position of MDT was defined by conducting a series of simulations using air as the working fluid. The simulation results also imply that the position of MDT is independent of selected working fluids.

To understand the thermal drift issue of convective accelerometer, the inner cylinder was controlled either as a constant heat flux heater or a constant differential temperature heater. The advantage of constant differential temperature heater is that the effect of the temperature-dependent thermal conductivity of working fluids can be eliminated.

A conventional solution provided by MEMSIC Corp. was introduced. The thermal drift of

convective accelerometer using air as the working fluid was reduced by using an outside compensation circuit. Relative low sensitivity error can be obtained by using different makes of thermistor. The introduction of the compensation circuit increases the cost of total system, and possibility to system failure as well.

Simulations of convective accelerometers using different working fluids were conducted and their performance was analyzed. Followed theoretical predictions in chapter 3, the thermal drift of convective accelerometer can be perfectly eliminated by using mercury as the working fluid. The simulation results also indicate the sensitivity change of convective accelerometers with the use of gas or liquid working fluids.

Chapter 4

Experimental Studies

A few convection-based microthermal accelerometer chips (MXR7210GL) fabricated by MEMSIC corporation were provided for our experimental study. The chips did not include an amplification circuit, so a high-accuracy instrumentation amplifier (AD620, Analog Device Corp.,) was selected to amplify the original tiny signal. To avoid any noise interference, the convection-based microthermal accelerometer and outside amplification circuit were located inside a metal box. The sensitivity and thermal drift of the convective accelerometer filled with different working fluids were documented and analyzed.

4.1   The Construction of Convective Accelerometer

The design principles of the convection-based microthermal accelerometer were presented in the first chapter. The applied acceleration can be deduced by the differential temperature of two temperature sensors. In Chapter 2, Equation (2.3) suggests that the position of maximum differential temperature is independent of the selected working fluid, i.e., the originally fabricated convective accelerometer which uses air as a working fluid can use other liquid working fluids to improve its sensitivity.

4.1.1   Operation of Prototype Convective Accelerometer

The prototype accelerometer chip was contained in a ten-pin-can package. It is shown in Figure 4.1. The convective accelerometer chip senses an applied acceleration orthogonal to the polysilicon heater. Pin 3 and pin 8 are connected to the power supply (CircuitSpecialists®
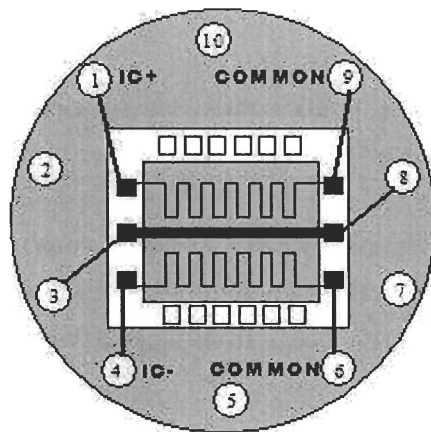
Figure 4.1: The Top View of Prototype Convective Accelerometer
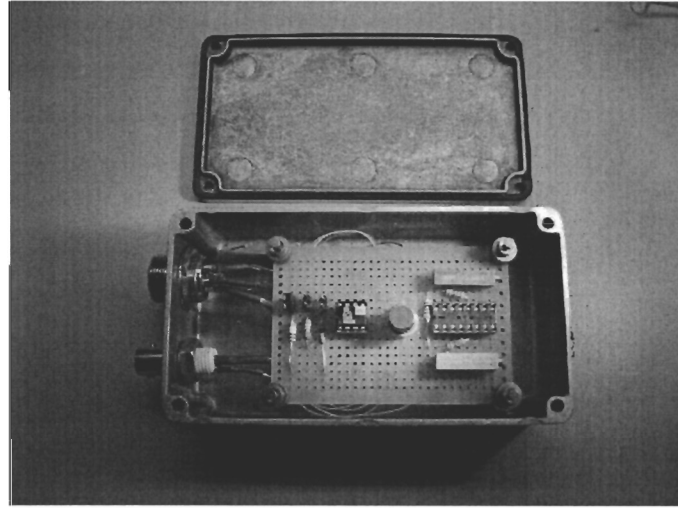
Figure 4.2: Accelerometer Circuitry Shielded by a Metal Box

CSI3003) and a voltage $5V$ put across them. The common mode signal can be detected either by the top thermopiles (pin 1 and pin 9) or bottom thermopiles (pin 4 and pin 6). The desired differential signal can be detected between pin 1 and pin 4. To a standard 1 g acceleration, the signal output of tested accelerometer chips using air as the working fluid is around 250 μV without any amplification. The applied acceleration can be deduced from the measured differential signal.

4.2   The Amplification Circuit

For the prototype convective accelerometer chips using air as the working fluid, the signal output is around a few hundred μV level when a standard 1 g acceleration was applied to the accelerometer. Such a tiny signal is very hard to measure by digital multimeter or oscilloscope. In this case, an outside amplification circuit is necessary to amplify this small differential signal.

In comparison with the tiny differential signal, outside noise can be easily picked up and amplified and then overwhelm the signal. Two solutions were applied to reduce the interference of noise. First, the accelerometer and amplification circuit needed to be properly grounded. Second, the whole circuit board which contains the accelerometer chip and amplification
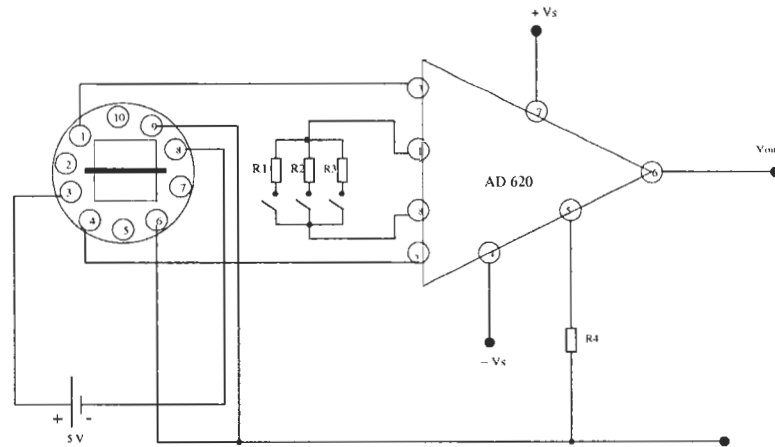
Figure 4.3: The Amplification Circuit for Convective Accelerometer

circuit was shielded inside a metal box, shown in Figure 4.2.

After careful consideration, the instrumentation amplifier AD620 [4] fabricated by Analog Device Corporation was selected and the amplification circuit shown in Figure 4.3 was built. Considering the sensitivity of different working-fluid-filled convective accelerometer, three external gain resistors (6193 Ω, 498.2 Ω, 49.69 Ω) were selected such that the differential signal can be amplified 10, 100 and 1000 times, respectively.

4.3 The Tilting Structure

The static 1 g acceleration applied to the convective accelerometer can be achieved by tilting the chip from horizontal to vertical position. For this project, a tilting structure was built so that the applied acceleration can vary from 0.1 g to 1 g. The metal box, which includes the convective accelerometer chip and amplification circuit, was located in the chassis of tilting structure. The tilting structure and environmental chamber are shown in Figure 4.4.

One part of tilting structure was located inside the environmental chamber and another part, located outside the environmental chamber, was used to record the tilting angle. To balance the weight of metal box, one piece of chunky wood was attached below the chassis. During the experiment, the power supply wires and signal output cable were passed through the venting hole in the left side of environmental chamber.
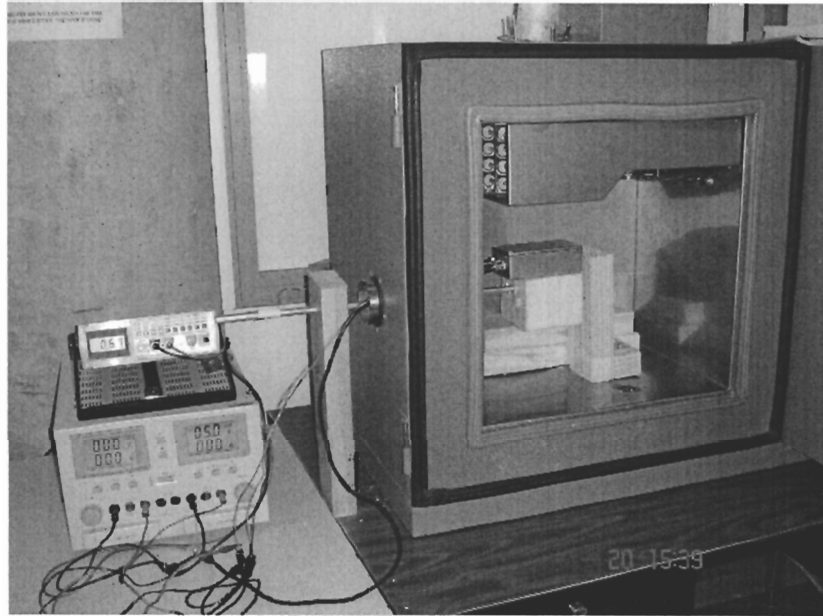
Figure 4.4: The Tilting Structure

4.4 The Performance of Convective Accelerometer

A few working fluids were selected for convective accelerometers. The sensitivity and thermal drift of convective accelerometers were documented and analyzed. Some important conclusions are drawn in this section. Also, one observation is that some electrically-conductive liquids are not suitable for the convective accelerometer.

4.4.1 Air as the Working Fluid

Air was selected as the initial working fluid for the convection-based accelerometer. The accelerometer was sealed at room temperature and put in the environment chamber (VersaTenn®). The gain resistor (49.69 Ω) was selected so that the amplification was set to 1000 times.

First, the temperature of environmental chamber was set to 273 K. It took a while for the signal output to become stable. A positive and negative gravitational acceleration were applied to the convective accelerometer. The signal output was documented when the loading chassis was tilted every 10 ° and the temperature of environment chamber was set at defined temperature. The differential signal was amplified 1000 times and the complete

Table 4.1: Experiment Results for Air-filled Convective Accelerometer (mV)

A.T.	273 K	293 K	313 K	333 K	353 K
-90°	384	284	198	140	110
-80°	376	279	195	138	108
-70°	357	265	186	131	101
-60°	325	244	171	121	93
-50°	285	217	152	107	82
-40°	237	182	123	88	65
-30°	185	142	99	69	52
-20°	123	96	66	47	36
-10°	61	47	34	23	17
0°	0	0	0	0	0
10°	-53	-40	-31	-20	-15
20°	-114	-87	-63	-47	-35
30°	-176	-132	-96	-67	-52
40°	-226	-170	-123	-88	-67
50°	-268	-201	-145	-105	-81
60°	-301	-231	-166	-122	-90
70°	-327	-246	-178	-132	-97
80°	-339	-255	-186	-138	-101
90°	-342	-257	-188	-140	-102
Sensitivity (mV/g)	363	271	193	140	106
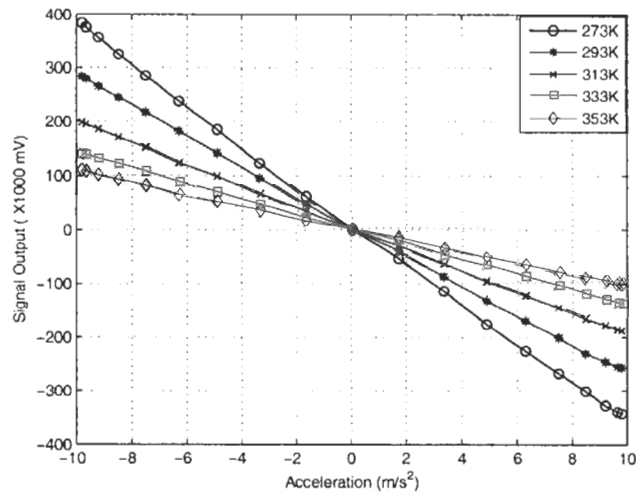
Figure 4.5: The Signal Output at Different Temperature for Air-filled Convective Accelerometer

experiment results are listed in Table 4.1. Note that *A.T.* in this table stands for Ambient Temperature, i.e., the temperature of environmental chamber.

The signal output of air-filled convective accelerometer at different temperature is plotted in Figure 4.5. Meanwhile, the sensitivity was calculated at different temperature in Table 4.1. The sensitivity change due to the ambient temperature change was plotted in Figure 4.6. A few conclusions can be drawn from the above experimental results:

- **Linearity**

  Figure 4.5 shows that very good linearity can be obtained by using air as the working fluid at different temperature.

- **High Sensitivity**

  Thanks to high accuracy amplification circuit, relative high sensitivity can be obtained from air-filled convective accelerometer. During the experiment, the air-filled convective accelerometer can sense the change of 5 degrees inclination at room temperature.

- **Thermal Drift**

  The sensitivity of air-filled convective accelerometer goes down when ambient temperature goes up. Also, the experimental results show that the sensitivity of air-filled
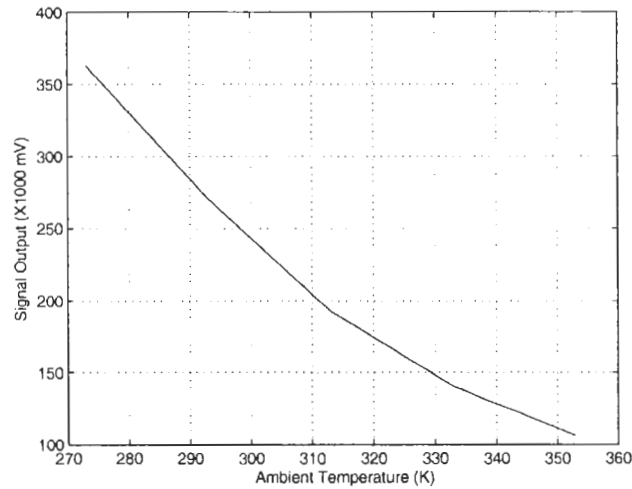
Figure 4.6: The Thermal Drift of Air-Filled Accelerometer

convective accelerometer at 273 K is about 3 times of sensitivity at 353 K, which agrees with the previous theoretical calculations and numerical simulations.

4.4.2   Liquid Working Fluids

The same accelerometer chip was used to test the performance of a liquid-filled convective accelerometer. It is straightforward to inject the liquid into the cavity of convective accelerometer. The metal cap was first removed from the accelerometer chip. A very fine syringe injected the liquid to the cavity and the metal cap individually, the accelerometer was then inverted and sealed using the metal cap.

Since some of the working fluids tested, such as methanol, are toxic, latex gloves and mask are recommended for the above procedures. To avoid cross-contamination of each working fluid, separate syringes were used for each working fluid. After the test of each working fluid, the remaining liquid in the accelerometer chip was rinsed completely by ether.

4.4.3   Silicon Oil as the Working Fluid

Silicon oil, a non-electrical-conductive liquid, was selected as the working fluid for the convective accelerometer. The gain resistor (498.2 Ω) was selected so that the amplification

Table 4.2: Experiment Results for Silicon Oil-filled Convective Accelerometer (mV)

A.T.	273 K	293 K	313 K	333 K	353 K
-90°	37.9	139	324	579.8	932
-80°	37.5	136	319	576.8	930
-70°	36.2	128	303	555.8	902
-60°	33.3	116	278	515.8	842
-50°	29.4	102	248	462.8	759
-40°	24.2	84	202	384.8	631
-30°	19.1	69	159	302.8	508
-20°	12.9	46	106	216.8	350
-10°	6.6	24	53	113.5	182
0°	0	0	0	0	0
10°	-6.2	-21	-52	-92.4	-174
20°	-12.7	-44	-104	-206.2	-352
30°	-19.2	-65	-164	-301.2	-507
40°	-24.5	-84	-206	-377.2	-642
50°	-29.3	-98	-246	-447.2	-746
60°	-33.5	-112	-275	-506.2	-841
70°	-36.4	-121	-293	-546.2	-898
80°	-38.1	-126	-304	-567.2	-927
90°	-38.7	-127	-305	-570.2	-929
Sensitivity (mV/g)	38.3	133	315	575	931

was set to 100 times. The complete experimental results are listed in Table 4.2.

The signal output of silicon oil-filled convective accelerometer for different gravitational accelerations at defined temperatures is plotted in Figure 4.7. The sensitivities at defined temperature are calculated and plotted in Figure 4.8. A few conclusions can be drawn from the above experimental results:

- **Linearity**
  Figure 4.7 shows that very good linearity can be obtained by using silicon oil as the working fluid.

- **High Sensitivity**
  During the experiment, we found that the tested accelerometer chip can sense even the change of 1 degree of inclination at room temperature. The sensitivity of the amplified
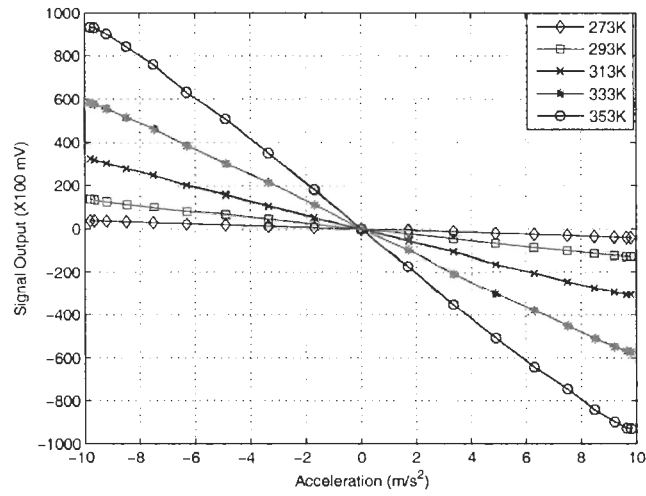
Figure 4.7: The Signal Output at Different Temperature for Silicon-Oil-filled Convective Accelerometer
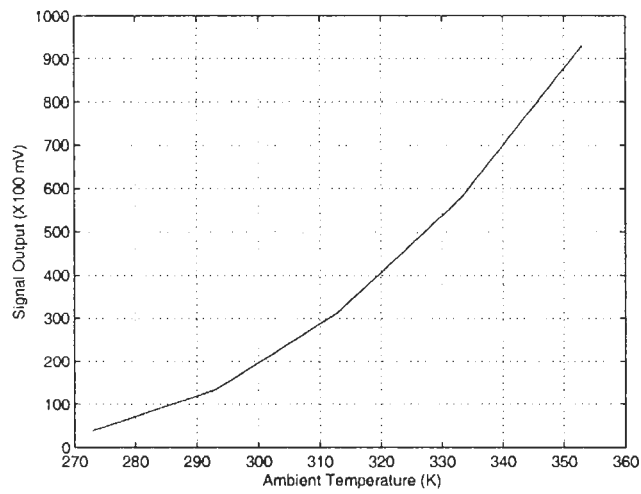
Figure 4.8: The Thermal Drift of Silicon Oil-Filled Accelerometer

output from the silicon oil-filled convective accelerometer at 293 K is 5 times higher than the sensitivity of air-filled convective accelerometer; and, since the signal from the air-filled chip is amplified 1000 times while the signal from the silicon oil-filled chip is only amplified 100 times, we can conclude that the MDT for the silicon oil-filled accelerometer is 50 times that of the air-filled accelerometer.

- **Thermal Drift**

  The sensitivity of silicon oil-filled convective accelerometer goes up when the ambient temperature goes up. The sensitivity at 353 K is about 25 times the sensitivity at 273 K.

4.4.4 Methanol as the Working Fluid

Theoretical calculations and numerical simulations both suggest that convective accelerometer filled with methanol can achieve very high sensitivity and acceptable thermal drift. However, due to its electrical-conductivity, methanol can not be used in this design. The methanol inside the accelerometer chip connects the positive bonding pad and the negative bonding pad directly.

Experimental study confirms this prediction. No valuable data can be achieved from the methanol-filled convective accelerometer. Two observations were obtained from a cleaned accelerometer chip filled with methanol:

- The signal output fluctuated randomly.

- Observed under the microscope, the surface colour of top and bottom thermopiles becomes green, and the initial colour of thermopiles was gold. This suggests a reaction is occurring between the fluid and the circuit materials.

Considering the above facts, mercury is not selected for use in this chip in the experimental study of convective accelerometers. The problems encountered with methanol suggest that, although mercury is predicted to perform well in numerical simulations, the chip structure must be re-designed before it can be tested experimentally.
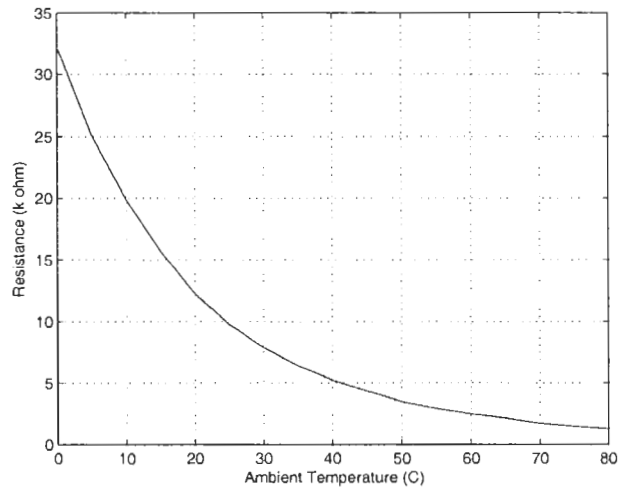
Figure 4.9: The Thermistor Performance

4.5 The Performance of Thermistor-Based Accelerometer

Due to the physical structure of the MEMSIC chips, electrically-conductive liquids can not used as potential working fluids. Another prototype, designed to work with conductive fluids, was built to test the thermal drift issue of convective accelerometers.

After careful comparisons, a high-sensitivity NTC thermistor (P/N: 7519) fabricated by U.S. SENSOR® was selected for this project. The performance of the thermistor is shown in Figure 4.9.

The convective accelerometer prototype is shown in Figure 4.10. Two thermistors are parallel aligned on either side of a nichrome wire heater. Both ends of the glass tube were sealed by two carved rubber stoppers. The fine nichrome wire passes along the axis of the glass tube and through the two stoppers.

4.5.1 Air is Selected as the Working Fluid

To test the performance of the prototype, air is first selected as the working fluid. The experimental results are shown in Table 4.3. 1 V voltage is put across the nichrome wire heater. Two accelerations, a positive and negative gravitational acceleration, were applied
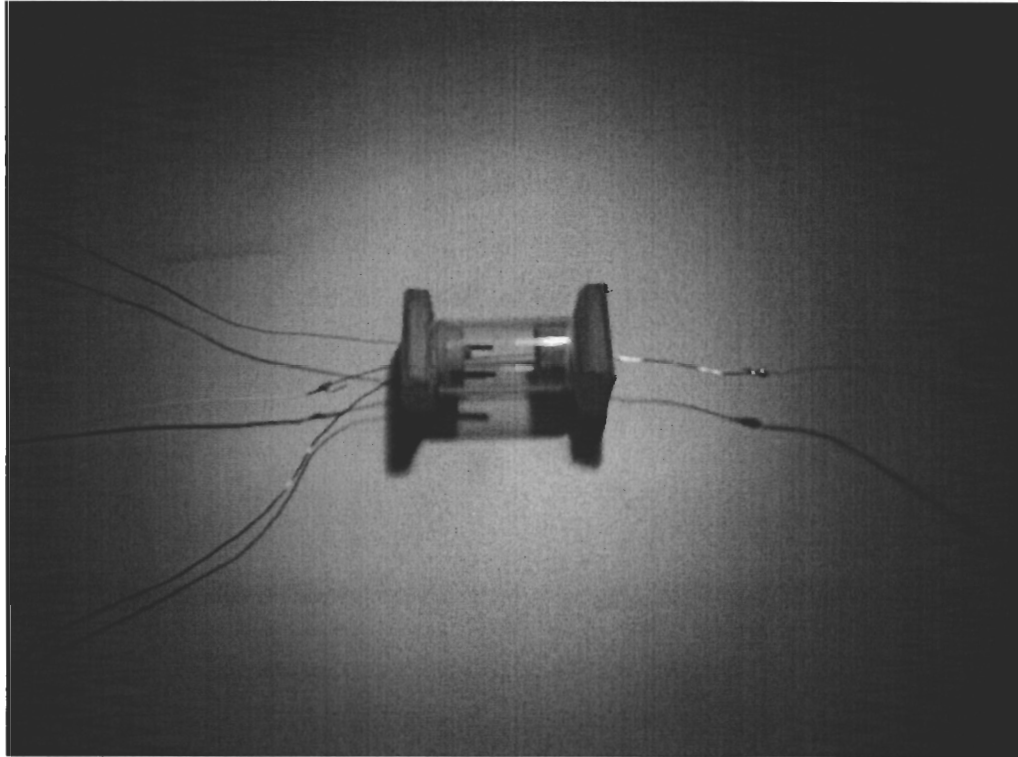
Figure 4.10: The Convective Accelerometer Prototype

Table 4.3: Experiment Results for Thermistor-Based Accelerometer Filled with Air

	The Thermistor Signal Output			
Ambient Temperature	$-g$	0	$+g$	Sensitivity
$^\circ C$	$^\circ C$			$^\circ C/g$
0	13.783	12.768	10.350	1.717
20	31.820	30.954	28.659	1.581
40	49.234	48.174	46.991	1.122
60	69.058	68.588	68.176	0.441
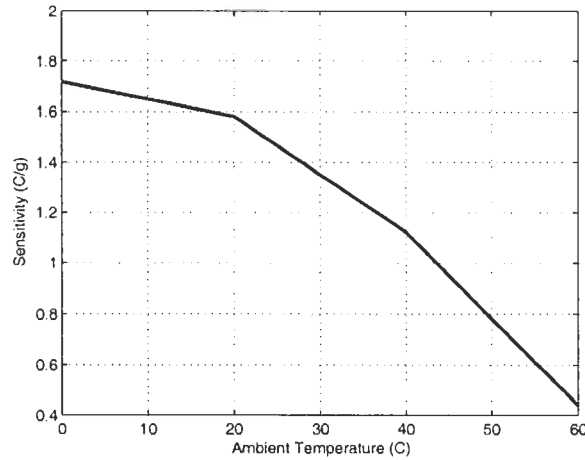
Figure 4.11: The Sensitivity of Thermistor-Based Accelerometer Filled with Air

to the prototype. To test the size of thermal drift, the temperature of environmental chamber was set at 0, 20, 40 and $60°C$, respectively. Note that the two rubber seals melt when the temperature is over $60°C$. For these experiments, the temperature at each thermistor was recorded as the accelerometer was rotated, and the difference between its maximum and minimum temperatures calculated. (This was done because it was difficult to place the thermistors symmetrically.) The signal outputs of two thermistors are plotted and shown in Figure 4.11.

A few observations can be achieved from the above experimental results.

- Sensitivity. The results show that the left thermistor can get higher sensitivity than that of the right thermistor, which can be explained by the different position of the two thermistors. Theoretically, the thermistor closer to the position of MDT can obtain higher sensitivity.

- Thermal Drift. The results show that the convective accelerometer also suffers from thermal drift. The sensitivity of the convective accelerometer goes down when ambient temperature goes up, which agrees with the conclusion of original convection-based microthermal accelerometer.

Table 4.4: Experiment Results for Thermistor-Based Accelerometer Filled with DI Water

	The Thermistor Signal Output		
Ambient Temperature	0	$-g$	Sensitivity
$^\circ C$	$^\circ C$		$^\circ C/g$
0	7.599	8.083	0.484
20	25.998	26.810	0.812
40	46.920	48.464	1.544
60	68.011	64.147	3.864
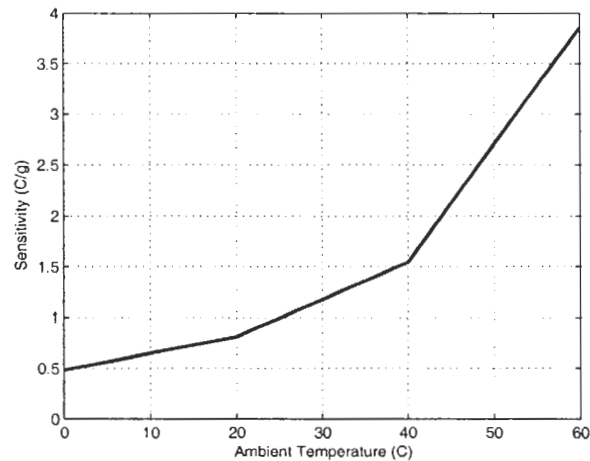
Figure 4.12: The Sensitivity of Thermistor-Based Accelerometer Filled with DI Water

4.5.2 DI Water as the Working Fluid

DI water was selected as the working fluid for the prototype. The experimental results were listed in Table 4.4. The sensitivities of thermistor-based accelerometer are plotted and shown in Figure 4.12. A few observations were obtained from the above results:

- Sensitivity. Compared with air-filled convective accelerometer prototype, relative higher sensitivity can be achieved by using DI water as the working fluid. The increase in sensitivity is smaller than the Rayleigh-number studies in Chapter 3 suggest. This may be due to several factors: the power supplied to the heater of water-filled chip was about half that supplied to the air-filled chip; the higher conductivity of water means that the heater temperature will be lower for a given heater power.

- Thermal Drift. The sensitivity of convective accelerometer filled with DI water goes up when ambient temperature goes up.

4.6 Conclusion

In this chapter, an amplification circuit was fabricated to pick up the tiny signal of convective accelerometer. To reduce noise effect, the circuit board and the chip were properly grounded and put inside a metal box. A tilting and supporting structure were made to test the performance of convective accelerometers filled with different working fluids.

Air and silicon oil were selected as the working fluid for convective accelerometers. The experimental results show that high sensitivity can be achieved by using air as the working fluid. The sensitivity of air-filled convective accelerometer goes down when ambient temperature goes up, which agrees with our prediction. The experimental results indicate that the sensitivity of silicon-oil filled convective accelerometer is much higher than that of convective accelerometer using air as the working fluid. The sensitivity of silicon-oil filled accelerometer goes up when ambient temperature goes up, which also agrees with our prediction.

Another convective accelerometer prototype was fabricated to further our study. The accelerometer prototype contains two high-sensitivity thermistors and a nichrome wire heater. The results show that the accelerometer prototype using DI water can achieve higher sensitivity than using air as the working fluid. The thermal drifts of the accelerometer prototype filled with air and DI water agree with previous study. Although the second prototype was designed for use with conductive liquids, we have not so far tested it with mercury or Galinstan. Placing mercury in a heated environmental chamber is an obvious health hazard. Galinstan is safe to use, but tends to stick to glass or metal walls unless they are specially prepared. A droplet of Galinstan was put on a microscope slide and a piece of aluminum foil which is shown in Figure 4.13.
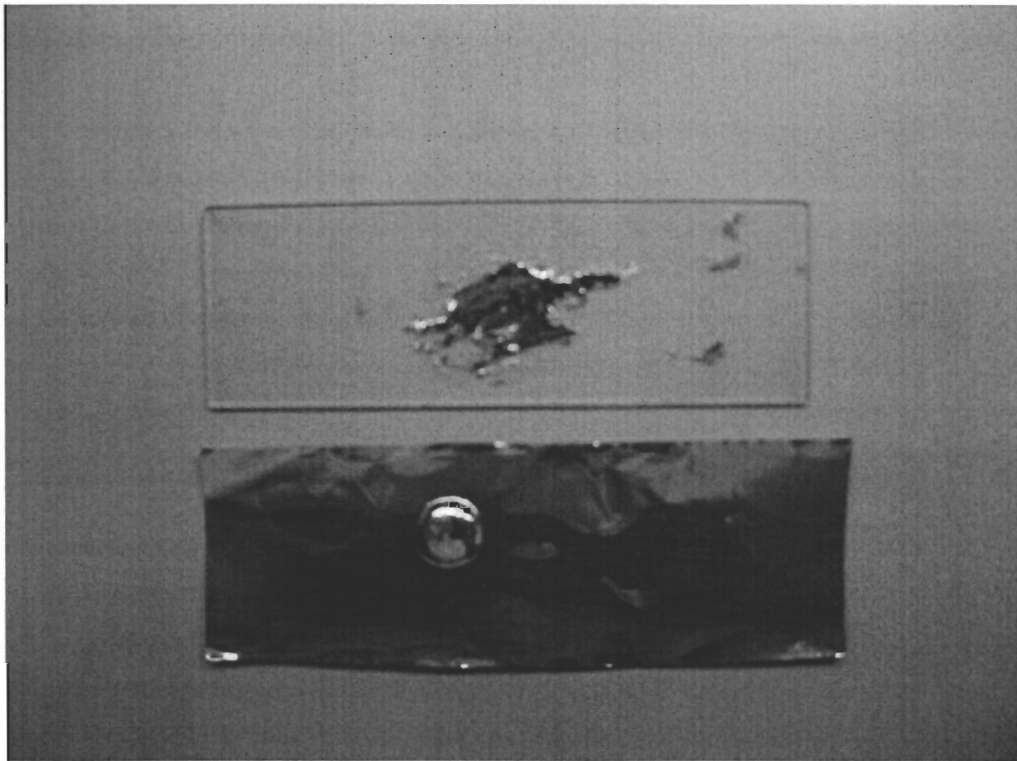
Figure 4.13: Galinstan on Glass Slide and Aluminum Foil

Chapter 5

Conclusions and Future Work

In this work, a few micromachined accelerometers, including some conventional accelerometers with proof-mass and unconventional accelerometers with no proof-mass, were introduced and their working theories were described. The performance of our research object, the convection-based microthermal accelerometer, was thoroughly analyzed. One of its disadvantages is thermal drift: the sensitivity changes rapidly as the ambient temperature changes. A recent numerical and experimental study has shown that the sensitivity of the convective accelerometer is a function of the Rayleigh number of the working fluid. Using this criterion, a few liquids were selected as potential working fluids to improve the sensitivity and to reduce the thermal drift of the convective accelerometer.

A variant of the original convective accelerometer, the convection-based heater-temperature accelerometer, was considered. Numerical simulations indicate that its sensitivity is three to four orders of magnitude lower than the original convective accelerometer with thermopiles, while it also suffers from thermal drift. The temperature in the heater to a standard gravitational acceleration was a few micro-Kelvin, which would be hard to measure experimentally.

Our research objective in this work is to reduce or eliminate the thermal drift of the convective accelerometer. A number of fluids, including air and some liquids, were selected as working fluids to analyze the performance of the convective accelerometer.

The physical properties of those selected working fluids at the defined temperature range were documented. The calculated Rayleigh number, Prandtl number and diffusivity were

used to predict the sensitivity and response time of different working-fluid-filled convective accelerometer. A FLOTRAN model of the convective accelerometer, a pair of concentric cylinders, was constructed for numerical simulations. The sensitivities of different working-fluid-filled convective accelerometer at the defined temperature range were normalized at 293 K and the results confirm that the thermal drift of convective accelerometer can be eliminated by using mercury as the working fluid.

A series of experimental tests were performed using an accelerometer chip developed by MEMSIC. Air and silicon oil were selected as the working fluids for this convective accelerometer. A few important observations were achieved, confirming prior theoretical calculations and numerical simulation results.

A second series of tests were performed using a thermistor-based accelerometer. Their results were consistent with theory. It is hoped that future work will demonstrate the use of mercury or Galinstan as a working fluid in this accelerometer. The toxicity of mercury makes experimental work potentially dangerous. Galinstan may be a safe substitute, but several material problems – its adhesion to glass and its ability to dissolve common metals – must be overcome before a prototype can be tested.

Appendix A

Hodnett's Solution

As mentioned in Chapter 3, the convection-based microthermal accelerometer can be modeled as a pair of infinitely long, horizontal, concentric cylinders. Many people contributed much valuable study to natural convection heat transfer between horizontal concentric cylinders. In 1973, there is a complete analysis presented by Patrick Hodnett to the temperature and velocity distributions of the concentric cylinder. The solution shows that the sensitivity of the convective accelerometer is a function of the Rayleigh number. By analyzing the definition of Rayleigh number, a few solutions were employed to improve the sensitivity of the accelerometer. Moreover, the reasons which lead to the thermal drift of the accelerometer were discovered.

A.1   Idealized Model and Assumptions

The mathematical model of the convective accelerometer was shown in Figure A.1. The inner cylinder stands for the polysilicon heater and the outer cylinder stands for the cavity of the accelerometer, respectively. The best locations for temperature sensors will be deduced from the solution of temperature distribution.

In this coordinate system:

T_o, r_o stand for the temperature and radius of outer cylinder, respectively.

T_i, r_i stand for the temperature and radius of inner cylinder, respectively.

r is the dimensionless distance along the radius.

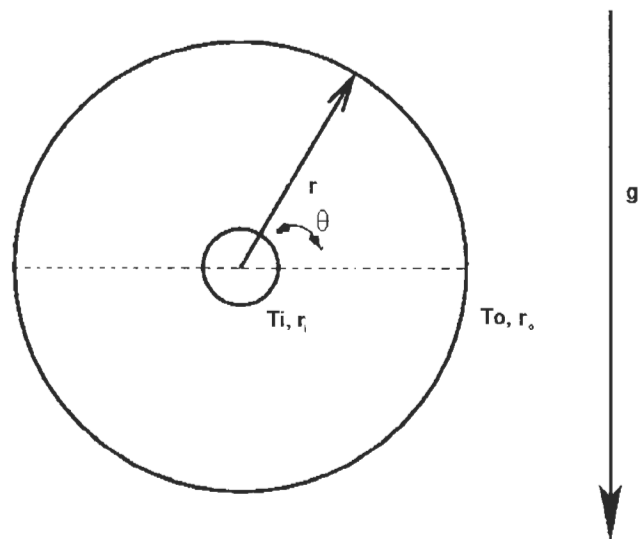θ is the angle between a given radius and the axis of acceleration.

Figure A.1: The Schematic of Design Principle

Patrick Hodnett made the following two assumptions before the calculation:

- The temperature difference between the cylinders is small such that ε is much less than 1.

- The radius of inner cylinder r_i is small such that the gravity number G is less than 1.

where: ε is the temperature difference between cylinders divided by the temperature of the outer cylinders: $\varepsilon = \frac{T_i - T_o}{T_o}$. G is the Gravity number defined by: $G = \frac{\rho^2 r_i^3 g}{\mu^2}$. Meanwhile, the above two assumptions also guarantee the Grashof number which is the product of ε and Gravity number is much less than 1.

A.2 Analytic Solution

Hodnett solved the governing equations by using perturbation method. The solution for the temperature distribution of concentric cylinder was shown in Equation A.1.

$$\frac{T}{T_0} = 1 + \varepsilon f_1(r) + m\varepsilon^2 f_2(r) + Ra\varepsilon f_3(r)\sin(\theta) + o(m\varepsilon^2, Ra\varepsilon) \tag{A.1}$$

where:

T_o is the temperature of the outer cylinder.

ε is the temperature difference between cylinders divided by the temperature of the outer cylinder, $\varepsilon = \frac{T_i - T_o}{T_o}$

R is the radius ratio, $R = r_o/r_i$.

Ra is Rayleigh number.

m is the parameter in $k \propto T^m$, in this study we assume $m = 0$.

And $f_1(r), f_2(r), f_3(r)$ are dimensionless functions of r and R only.

$$f_1(r) = 1 - (\ln r / \ln R) \tag{A.2}$$

$$f_2(r) = \frac{1}{2}\frac{\ln r}{\ln R}[1 - \frac{\ln r}{\ln R}] \tag{A.3}$$

$$f_3(r) = L_1 r + M_1 r^{-1} + \ln^{-1} R[\frac{1}{2}A_1 r \ln r - \frac{1}{2}B_1 r^{-1}\ln r + \frac{1}{8}C_1 r^3 +$$
$$\frac{1}{4}D_1 \ln r((\ln r - 1) - (r^3 \ln(r - \frac{3}{4})))]/(128\ln R) \tag{A.4}$$

where:

$$L_1 = -\ln^{-1} R(R^2 - 1)^{-1} [\frac{1}{2} A_1 R^2 \ln R - \frac{1}{2} B_1 \ln R + \frac{1}{8} C_1 (R^4 - 1) +$$
$$\frac{1}{4} D_1 R^2 \ln R(\ln R - 1) - (R^4 \ln R - \frac{3}{4} R^4 + \frac{3}{4})/(128 \ln R)] \qquad (A.5)$$

$$M_1 = \ln^{-1} R(R^2 - 1)^{-1} [\frac{1}{2} A_1 R^2 \ln R - \frac{1}{2} B_1 \ln R + \frac{1}{8} C_1 R^2 (R^2 - 1) +$$
$$\frac{1}{4} D_1 R^2 \ln R(\ln R - 1) - R^2 (R^2 \ln R - \frac{3}{4} R^2 + \frac{3}{4})/(128 \ln R)] \qquad (A.6)$$

$$A_1 = \frac{(\ln R)^{-1} R^2}{16[4R^2((R^2 - 1)^2 - (R^4 - 1) \ln R)]} [-R^6 + R^4 +$$
$$R^2 - 1 - 2(R^2 - 1)^2 \ln R + 8R^4 (\ln R)^2] \qquad (A.7)$$

$$B_1 = \frac{(\ln R)^{-1} R^4}{16[4R^2((R^2 - 1)^2 - (R^4 - 1) \ln R)]} [(R^2 - 1)^2 - 4R^2 (\ln R)^2] \qquad (A.8)$$

$$C_1 = \frac{(\ln R)^{-1} R^2}{16[4R^2((R^2 - 1)^2 - (R^4 - 1) \ln R)]} [(R^2 - 1)^2 +$$
$$2(R^2 - 1)^2 \ln R - 4R^4 (\ln R)^2] \qquad (A.9)$$

$$D_1 = \frac{(\ln R)^{-1} R^2 (R^2 - 1)}{8[4R^2((R^2 - 1)^2 - (R^4 - 1) \ln R)]} (R^4 - 1 - 4R^2 \ln R) \qquad (A.10)$$

Based on Lin's thesis, the dimensionless differential temperature, $\delta T/T_o$, measured by the accelerometer corresponds to the fourth term in Equation (A.1), $Ra\varepsilon f_3(r) \sin(\theta)$. Therefore, the differential temperature for radially opposite points at a given r is:

$$\delta T = 2RaT_0 \varepsilon f_3(r) \qquad (A.11)$$

Equation (A.11) implies that the sensitivity of the convection-based microthermal accelerometer is proportional to the Rayleigh number. ε, which is the temperature difference between cylinders divided by the temperature of the outer cylinder, can be substituted in Equation (A.11), which becomes:

$$\delta T = 2Ra\triangle T f_3(r) \qquad (A.12)$$

Appendix B

Complete Simulation Procedures In ANSYS

As mentioned in Chapter 4, the convection-based microthermal accelerometer can be modeled as a concentric cylinders by using the CFD program 'FLOTRAN'. Considering the complicated process to build the FLOTRAN model and the large number of parameters defined, the complete simulation procedures are described in this appendix as a guide for subsequent researchers.

B.1   Preprocessor

Starting 'ANSYS' in a terminal window and defined the class of problem as 'FLOTRAN CFD'. A FLOTRAN model was constructed and carefully meshed in this section. The detailed steps are described in the following.

1. Element Type

   The element type '2D FLOTRAN 141' is selected for meshing the model.

2. Modeling

   Since the straight line can not be defined in the concentric cylinder model directly, the left-side half annulus is first constructed. The complete model was built by reflecting the left half to the right half.

   Go to the option: Modeling > Create > Areas > Circle > Partial Annulus

   Define the parameters as follows and the partial annulus was shown in Figure B.1
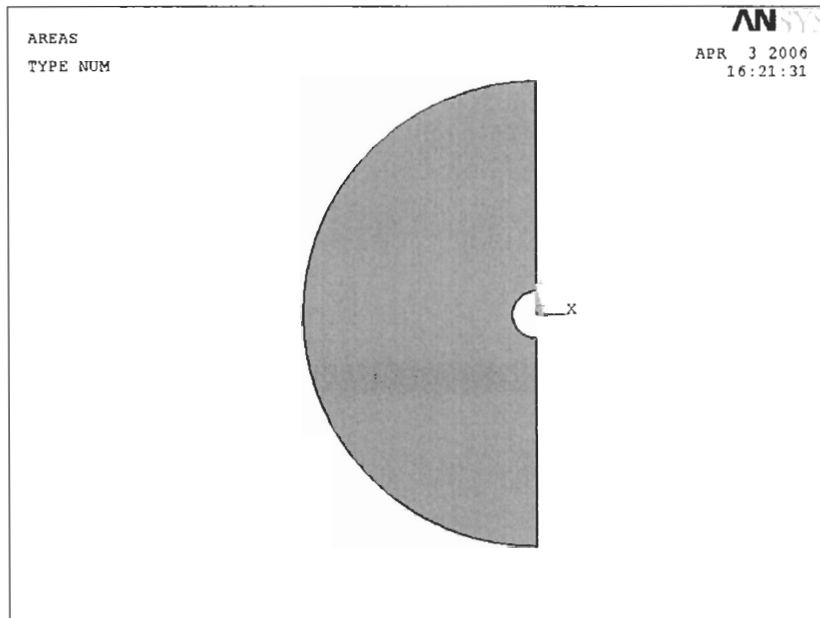
Figure B.1: The Partial Annulus

```
WP X    = 0
WP Y    = 0
Rad-1   = 0.0001
Theta-1 = 90
Rad-2   = 0.001
Theta-2 = 270
```

3. Meshing

    The meshing element size was varied from the finest meshing (1 μm in the straight line and 1 degree in the arc line) to the most coarse meshing (5 μm in the straight line and 5 degrees in the arc line). The simulation results showed that the mesh criterion (3 μm and 3 degrees) was fine enough to get accurate result.

    - Meshing > Size Controls > Manual Size > Lines > Picked Lines
      It defines the mesh criterion to the straight lines and arc lines. To the arc line, 3 degrees was set to the division arc. To the straight line, 0.00003 m was set to the element edge length and 10 to the space ratio.
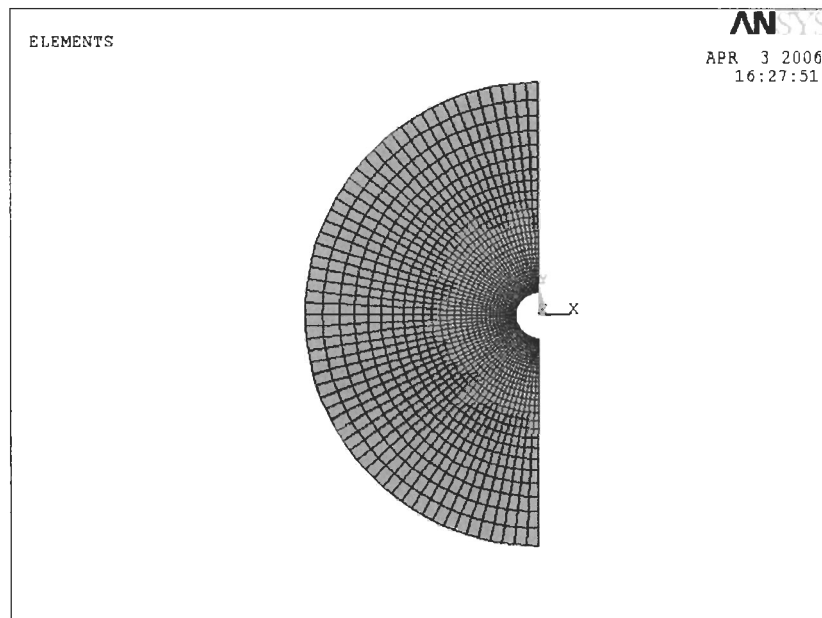
Figure B.2: The Meshed Annulus

- Meshing > Size Controls > Manual Size > Lines > Flip Bias
  The outside area around the inner cylinder was meshed more finely than the inner area around the outer cylinder.

- Meshing > Mesh Tool
  The left-side annulus was meshed and showed in the figure B.2.

4. Modeling and Coupling

  - Modeling > Reflect > Areas

  - Coupling/Ceqn > Coincident Nodes
    The tolerance for coincidence was set to $1.0*10^{-7}$. The meshed model is shown in Figure B.3. In course of building a FLOTRAN model, we may accidentally define multiple modes with identified locations. FLOTRAN must be told explicitly that these nodes are identical.

5. Loads

  - Loads > Define Loads > Apply > Thermal > Temperature > On Lines
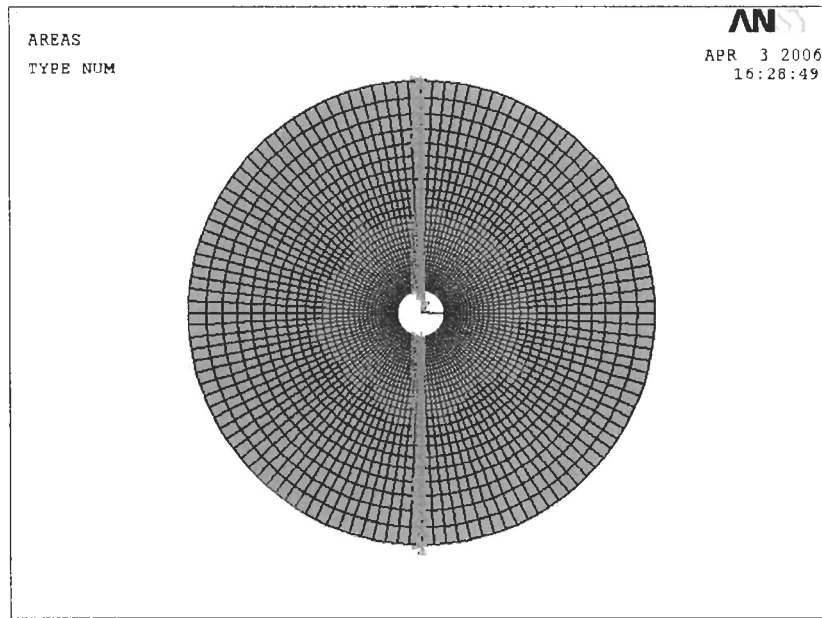
Figure B.3: The Meshed Concentric Model

The temperature of the outer cylinder is ambient temperature. To investigate the thermal drift, the temperature of the outer cylinder is set at 273 K, 293 K, 313 K, 333 K and 353 K.

- Loads > Define Loads > Apply > Thermal > Heat Flux > On Lines
  The heat flux value was calculated by using Equation (3.1) and (3.2).

- Loads > Define Loads > Apply > Fluid/CFD > Velocity > On Lines
  The velocity to the X and Y direction were 0.

B.2 Solution

1. FLOTRAN Set Up > Solution Options
   It is a problem about heat transfer.

2. FLOTRAN Set Up > Execution Ctrl
   The general termination criteria is set as the following:

   ```
   Pressure:    1e-02
   Temperature: 1e-08
   ```

3. FLOTRAN Set Up > Fluid Properties

   FLOTRAN has properties for air and water on file, but properties of other fluids must be entered manually.

4. FLOTRAN Set Up > Flow Environment > Gravity

   The acceleration is set as 10 m/s^2 toward the positive X direction.

5. FLOTRAN Set Up > CFD Solver Controls

   ```
   VX Solver CFD -- TDMA
   VY Solver CFD -- TDMA
   VZ Solver CFD -- TDMA
   PRES Solver CFD -- Precond con grad
   TEMP Solver CFD -- TDMA
   ```

6. Run FLOTRAN

   The simulation begins when all the boundary conditions and loading vector were set.

B.3   General Postprocessor

1. Read Results > Last Set

2. Plot Results > Contour Plot > Nodal Solution

   The temperature distribution of convective accelerometer was shown in Figure B.4.

3. Plot Results > Vector Plot > Predefined

   The velocity distribution was shown in Figure B.5.

4. Path Operations > Define Path > By Nodes

   The two paths, x_1 and x_2, are defined in Figure B.6.

5. Path Operations > Plot Path Item > List Path Items

   Two commands are used to show accurate results of temperature distribution along the path. If the working fluid is gas, such as air, the command '$/FORM,,G,18,11$' is used to show more decimal digits. If the working fluid is liquid, such as DI water, the command '$/FORM,,F,18,11$' is used.
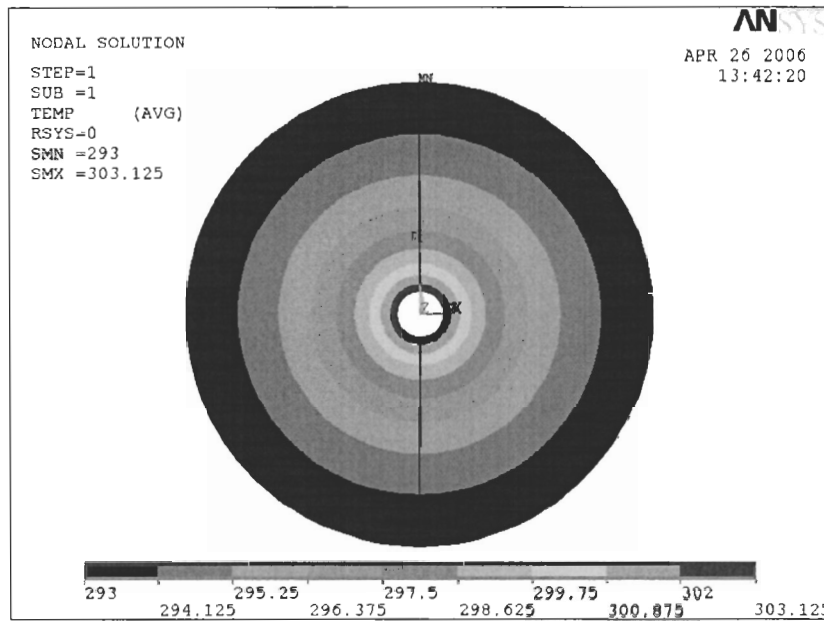
Figure B.4: Temperature Distribution of Convective Accelerometer

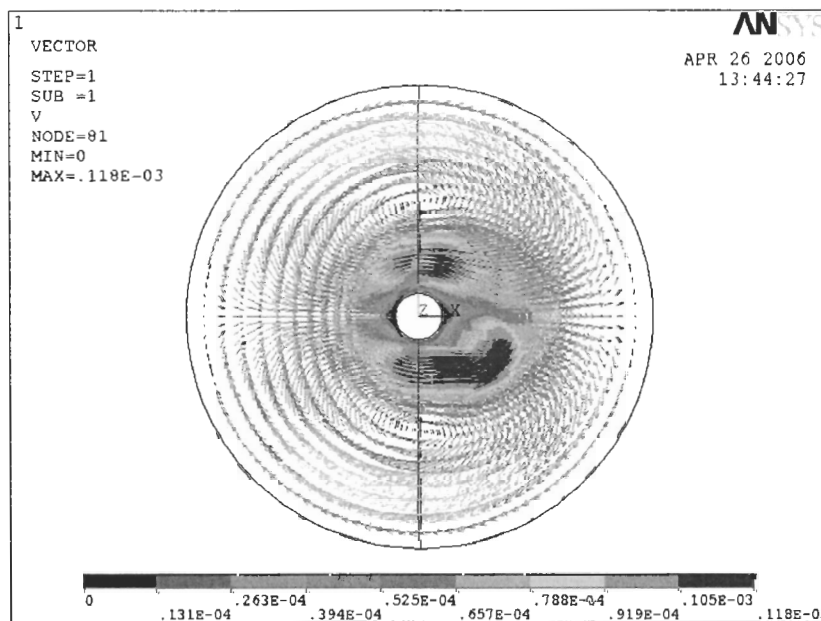
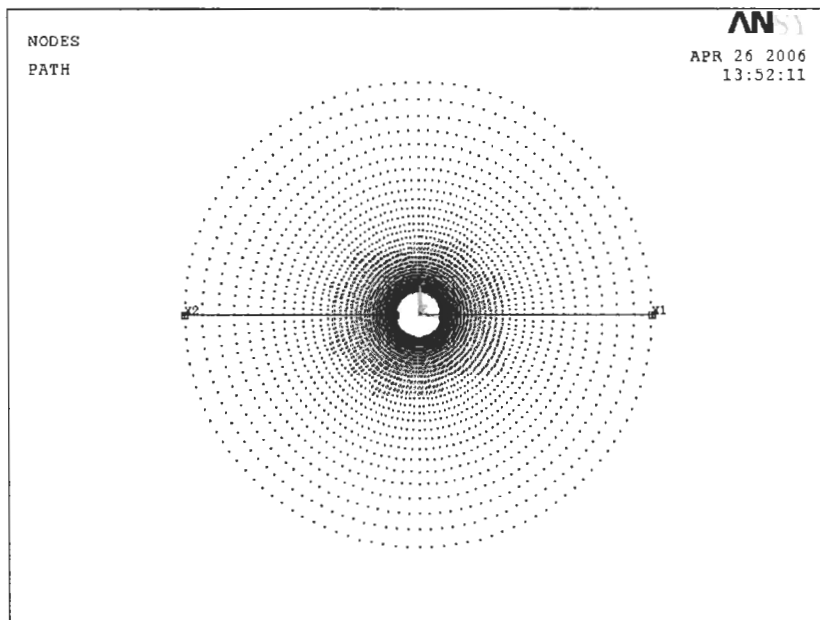Figure B.5: Velocity Distribution of Convective Accelerometer

Figure B.6: The Defined Two Paths

Bibliography

[1] A. B. Wu, J. Jones, *Analysis of Liquid-Filled Convective Micromachined Accelerometer*, International Conference for Upcoming Engineers, Waterloo, Ontario, May 2006

[2] A. B. Wu, J. Jones, *Thermal Drift of Convection-Based Microthermal Accelerometer*, ASME International Mechanical Engineering Congress and Exposition, Seattle, Washington, November 2007

[3] A. Leung, J. Jones, E. Czyzewska, J. Chen, and M. Pascal, *Micromachined Accelerometer with no Proof Mass*, in Technical Digest of Int. Electron Device Meeting (IEDM97), Washington, D.C., Dec. 1997, pp899-902.

[4] ANALOG DEVICES, *Low Cost Low Power Instrumentation Amplifier AD620*, http://www.analog.com, consulted November, 2004

[5] ANALOG DEVICES, *Monolithic Accelerometer With Signal Conditioning*, http://www.analog.com/UploadedFiles/Obsolete_Data_Sheets/2044696ADXL50.pdf, consulted November, 2005

[6] F. Kreith, *Principles of Heat Transfer*, Third Edition, New York, N.Y. USA, 1976 Impression, Harper & Row

[7] L. Lin, J. Jones, *A Liquid-Filled Buoyancy-Driven Convective Micromachined Accelerometer*, Journal of Microelectromechanical Systems, Vol. 14, No. 5, October 2005

[8] L. Lin, *Design and Analysis of Microthermal Accelerometer*, Ph.D Thesis, Simon Fraser University, March 2004

[9] Min-Hang Bao, *Micro Mechanical Transducers: Pressure Sensors, Accelerometers and Gyroscopes*, Elsevier, 2000.

[10] P. Hodnett, *Natural convection between horizontal heated concentric circular cylinders,* Journal of Applied Mathematics and Physics, vol. 24, pp.507-516, Nov. 1973

[11] R. Hiratsuka, D. C. van Duyn, T. Otaredian, P. de Vries and P. M. Sarro *Design Considerations for the Thermal Accelerometer,* Sensors and Actuators A, 32(1992) 380 - 385

[12] R. Hiratsuka, D. C. Van Duyn, T. Otaredian and P. de Vries *A Novel Accelerometer Based on a Silicon Thermopile* , Tech. Digest, 6th Int. Conf. Solid-State Sensors and Actuators (Transducers '91), San Francisco, CA, USA, June 24 - 27, 1991, pp. 420 - 423

[13] S. M. Sze, *Semiconductor Sensors,* John Wiley & Sons, Inc., New York, NY, 1994.

[14] W. H. Hoather, *The Density and Coefficient of Expansion of Liquid Gallium over a Wide Range of Temperature,* 1936, Phys. Soc. 48 pp.699-707

[15] *Galinstan Safety Data Sheet,* http://www.rgmd.com/msds/msds.pdf, consulted April, 2007.

[16] William S. Janna, *Introduction To Fluid Mechanics*, PWS-KENT Publishing Company, Boston, 1993.

[17] Richard J. Goldstein, *Fluid Mechanics Measurements* Second Edition, Taylor & Francis Ltd., USA, 1996.

[18] MEMSIC Application Note, #AN-00MX-001, *Accelerometer Fundamentals,* http://www.memsic.com, consulted April, 2005.

[19] MEMSIC Application Note, #AN-00MX-002, *Thermal Accelerometers Temperature Compensation,* http://www.memsic.com, consulted April, 2005.

[20] MEMSIC Application Note, #AN-00MX-003, *Thermal Accelerometers Frequency Compensation,* http://www.memsic.com, consulted April, 2005.

[21] MEMSIC Application Note, #AN-00MX-007, *Inclination Sensing with Thermal Accelerometers,* http://www.memsic.com, consulted April, 2005.

[22] MEMSIC Application Note, #AN-00MX-008, *Electrostatic Protection For Semiconductor Products,* http://www.memsic.com, consulted April, 2005.

[23] MEMSIC Application Note, #AN-00MX-009, *Using MEMSIC MXR2312GL/MXD2125GL In Car Alarm Applications,* http://www.memsic.com, consulted April, 2005.

[24] MEMSIC Application Note, #AN-00MX-012, *Inclination Sensing of Moving Vehicle,* http://www.memsic.com, consulted April, 2005

[25] MEMSIC Application Note, #AN-00MX-013, *Accelerometer Supported Tilt as an Input Method fo Mobile Devices,* http://www.memsic.com, consulted April, 2005.

[26] MEMSIC Application Note, #AN-00MX-014, *Low g Accelerometer Non-Linearity Measurement,* http://www.memsic.com, consulted April, 2005.

[27] MEMSIC Application Note, #AN-00MX-015, *Inclination Sensing of Digital Projector for Correction of Image Distortion and Inversion,* http://www.memsic.com, consulted April, 2005.

[28] X. B. Luo, Y. J. Yang, F. Zheng, Z. X. Li and Z. Y. Guo, *An Optimized Micromachined Convective Accelerometer with no Proof Mass,* Journal of Micromechanics And Microengineering, Vol. 11, pp 504-508, 2001.

[29] *Handbook of CHEMISTRY and PHYSICS,* 87th Edition, 2006 - 2007, http://www.hbcpnetbase.com, consulted February, 2005.

[30] *Physical Properties of Sulfur Hexafluoride,* http://home.earthlink.net/ jimlux/hv/sf6.htm, consulted April, 2005.

[31] Bhalchandra V. Karkekar, Robert M. Desmond, *Engineering Heat Transfer,* West Publishing Company, St. Paul, Minn, 1982.

[32] *Crossfire Commander (Beilstein Database),* http://www.lib.sfu.ca/researchtools/databases/dbofdb.htm?DatabaseID=168, consulted February, 2005.